Journal of Geodynamics 65 (2013) 94–116

Contents lists available at SciVerse ScienceDirect

Journal of Geodynamics

journal homepage: http://www.elsevier.com/locate/jog

Structural evidence for strike-slip deformation in the İzmir–Balıkesir transfer zone and consequences for late Cenozoic evolution of western Anatolia (Turkey)

Bora Uzel[a,*], Hasan Sözbilir[a], Çağlar Özkaymak[a], Nuretdin Kaymakcı[b], Cornelis G. Langereis[c]

[a] Dokuz Eylül University, Department of Geological Engineering, Buca, TR-35160 İzmir, Turkey
[b] Middle East Technical University, Department of Geological Engineering, TR-06531 Ankara, Turkey
[c] Utrecht University, Fort Hoofddijk Paleomagnetic Laboratory, 3584-CD Utrecht, The Netherlands

ARTICLE INFO

Article history:
Received 3 January 2012
Received in revised form 13 June 2012
Accepted 16 June 2012
Available online 4 July 2012

Key words:
Strike-slip tectonics
Fault kinematics
Palaeostress inversion
İzmir Bay
İzmir–Balıkesir transfer zone
Western Anatolia

ABSTRACT

The İzmir–Balıkesir transfer zone (İBTZ) is a recently recognized strike-slip dominated shear zone that accommodates the differential deformation between the Cycladic and Menderes core complexes within the Aegean Extensional System. Here, we present new structural and kinematic data obtained from field observations and 1/25,000 scale mapping of Miocene to Recent units within the İBTZ around İzmir Bay. The results point out that the İBTZ is a transtensional brittle shear zone that affects the pre-Neogene basement rock units, the early-middle Miocene volcano-sedimentary units and the Plio–Quaternary continental units.

The analysis of large-scale structures and fault kinematic data indicate that three different deformation phases prevailed in the İzmir Bay region during the late Cenozoic. The first phase (Phase 1) is characterized by N–S directed extension and E–W contraction that gave way to the development of strike-slip faults with normal components and likely took place during the early (?) to late Miocene. This transtensional phase, forming the volcano-sedimentary basin of deposition was overprinted by the second phase (Phase 2) which is characterized by variable extension and contraction directions indicating wrench- to extension-dominated transtension. The structures related to Phase 2 are observed all around the İzmir Bay and indicate a distributed nature of the deformation that probably took place during the early Pliocene, coeval with the end of the activity of the Mid-Cycladic Lineament and the last exhumation of the central Menderes Massif. The latest deformation phase (Phase 3) is characterized by an association of NW–SE trending left-lateral and NE–SW trending right-lateral strike-slip faults and E–W trending normal faults forming transtensional deformation. During Phase 3, the İBTZ evolved from a wider shear zone into a relatively narrow discrete fault zone by the late Pliocene, during which the strike-slip and extensional deformation were completely decoupled from each other. The field-based evidence for strike-slip deformation from the region has only recently been recognized, but has very important implications for understanding the deformation styles and coupling of Aegean–West Anatolian extensional deformation system along the İBTZ. We conclude that the İzmir Bay Basin developed during the Plio–Quaternary within the dextral İBTZ.

1. Introduction

The Cenozoic deformation and related basin formation in western Anatolia is one of the hot topics in geoscience research in the active Africa–Europe convergence zone. This is mainly due to the complex deformation history of the region where metamorphism, basin formation and volcanism took place coevally. Şengör et al. (1985), Bozkurt (2001, 2003), and Ersoy et al. (2010) have discussed and summarized the main ideas on Cenozoic tectonics and related basin formation history in this (mainly) extensional system. Despite the large number of studies in the region that include many aspects of tectonics, only few appreciated the importance of strike-slip deformation in western Anatolia, except the early studies of Kaya (1979, 1981), and Şengör (1987), and the more recent studies of, Ring et al. (1999), Özkaymak and Sözbilir (2008), Uzel and Sözbilir (2008), Sözbilir et al. (2009, 2011) and Uzel et al. (2012). In particular, Uzel and Sözbilir (2008) provided convincing evidence for the existence of a major strike-slip zone in the region, the İzmir–Balıkesir Transfer Zone (İBTZ), which accommodates differential extensional strain between the Cycladic Core Complex in the southwest and the Menderes Core Complex in the northeast (Fig. 1). This NE-trending transfer zone includes a number of secondary strike-slip faults striking generally NE–SW and NW–SE, and

* Corresponding author. Fax: +90 2324127300.
E-mail address: bora.uzel@deu.edu.tr (B. Uzel).

0264-3707/$ – see front matter © 2012 Elsevier Ltd. All rights reserved.
http://dx.doi.org/10.1016/j.jog.2012.06.009

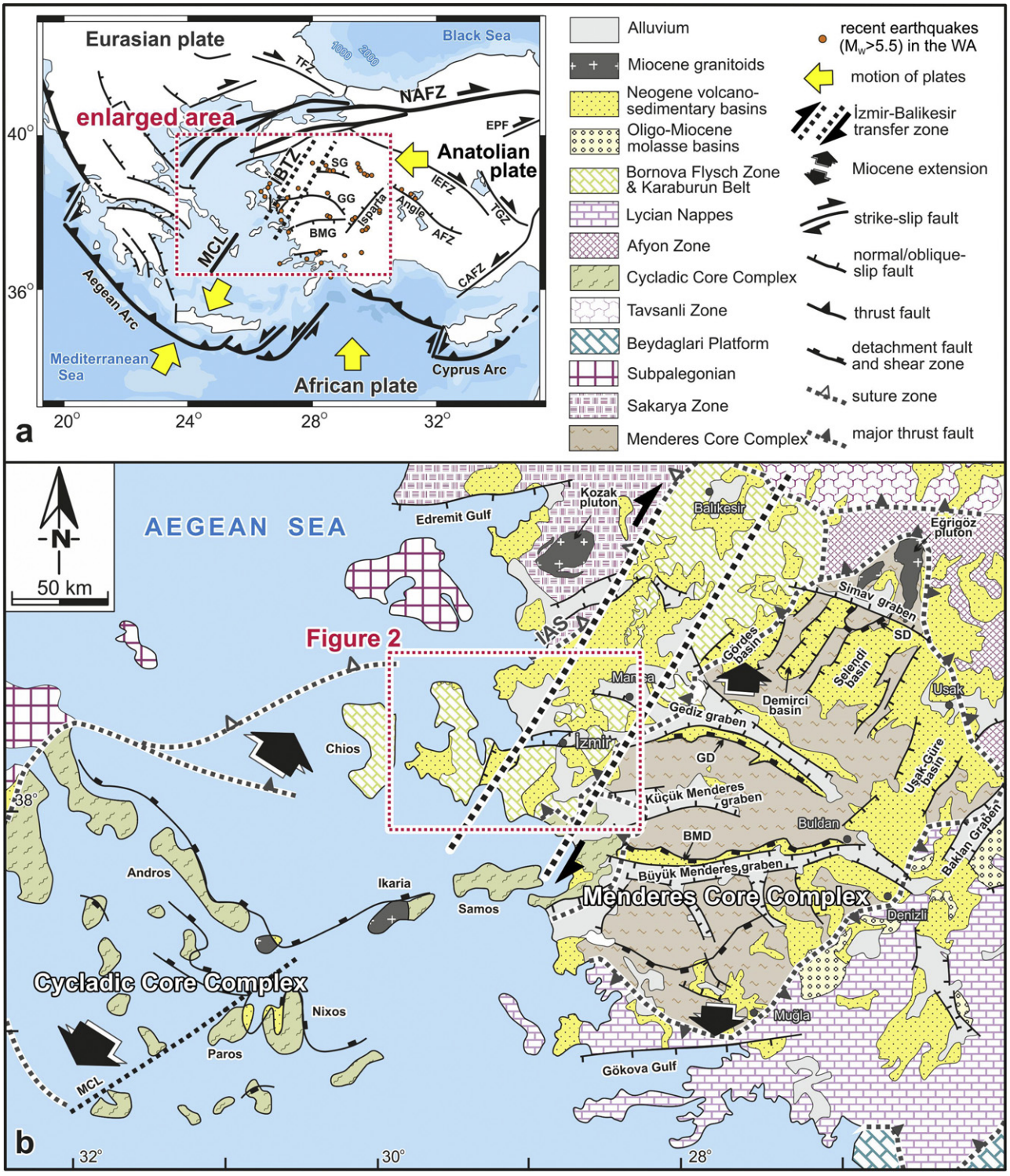

Fig. 1. (a) Simplified map showing the major (plate) tectonic elements and configuration of the Aegean region. NAFZ, North Anatolian fault zone; CAFZ, Central Anatolian fault zone; EPF, Ezinepazarı Fault; TGF, Tuz Gölü Fault; İEFZ, İnönü-Eskişehir fault zone; AFZ, Akşehir fault zone; G, Gökova Bay; BMG, Büyük Menderes Graben; GG, Gediz Graben; SG, Simav Graben; TFZ, Thrace fault zone (redrawn from Taymaz et al., 2007 and compiled from Koçyiğit and Özaçar, 2003; Kaymakçı et al., 2007 and our observations). The seismic data for western Anatolia (WA) are from Tan et al. (2008). b) Simplified tectonic map of western Anatolia (after Sözbilir et al., 2011). GD, Gediz Detachment Fault; BMD, Büyük Menderes Detachment Fault; İAS, İzmir–Ankara Suture Zone.

normal faults striking E–W, which are seismically active and control the evolution of several Miocene to Recent sedimentary basins (Emre et al., 2005; Uzel and Sözbilir, 2008; Uzel et al., 2012; Sözbilir et al., 2011).

The central part of the İBTZ is the İzmir Bay which is one of the most distinctive bays in the Aegean Sea in having a "boot-shaped" geometry with Karaburun Peninsula defining its western–northwestern boundary, while the Foça-Yuntdağı and Yamanlar highs delimit it from the north-northeast. The southern boundary is defined by the Seferihisar and Nifdağı highs. It is an approximately 10–20 km wide and 50–60 km long depression (Fig. 2). Topographically and bathymetrically it comprises two

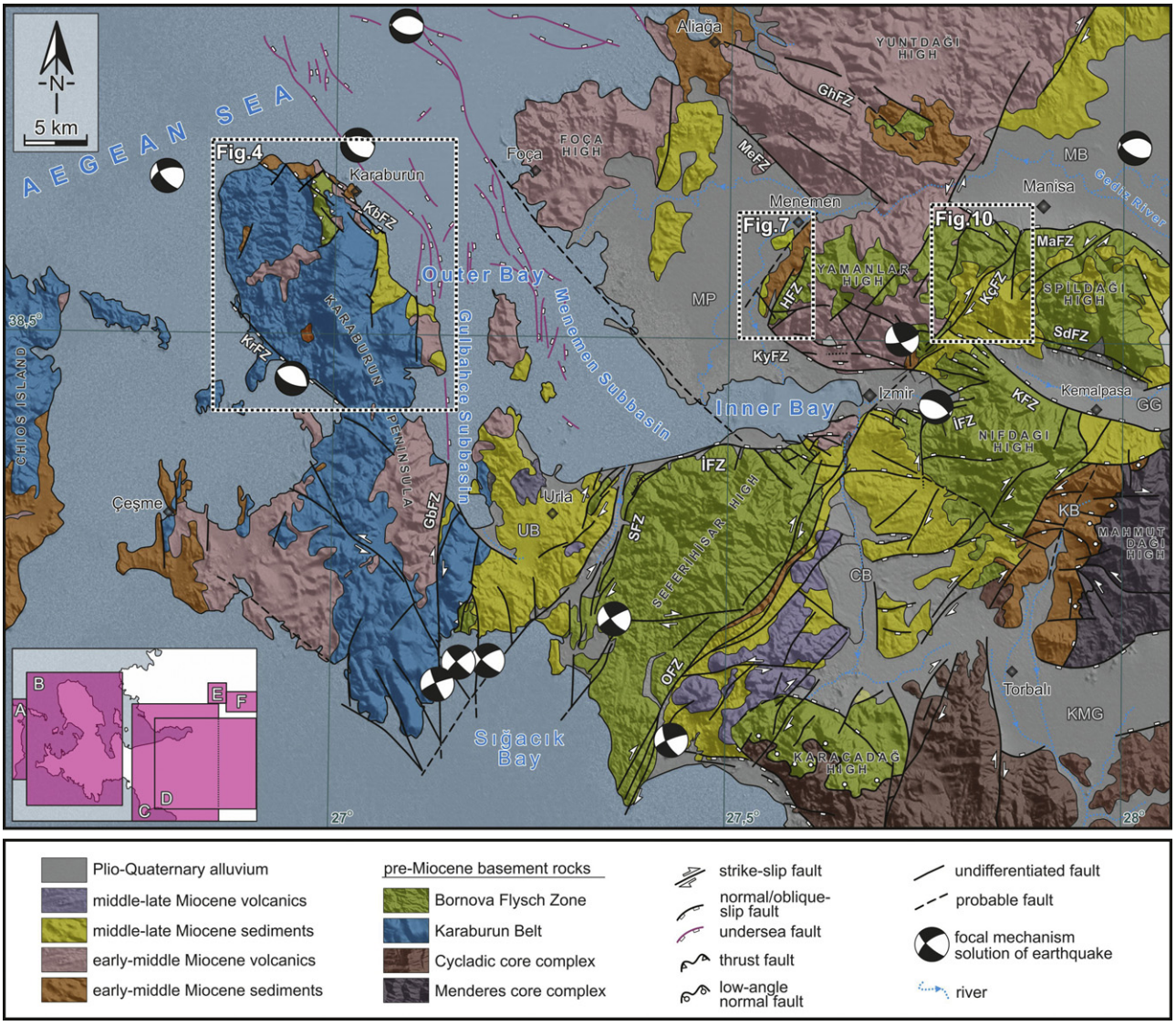

Fig. 2. Simplified geological map of İzmir Bay area draped on topographic data. Reference geological maps are after (A) Pe-Piper et al. (1995), (B) Çakmakoğlu and Bilgin (2006), (C) Uzel et al. (2012), (D) Sözbilir et al. (2011), (E) Özkaymak et al. (2011), (F) Bozkurt and Sözbilir, 2006); A–F are indicated in the lower-left inset map. Lower hemisphere equal area projection plots of the focal mechanism solutions of main earthquakes are taken from the Earthquake Catalogues for Turkey (Tan et al., 2008); the black (white) parts are compressional (extensional) quadrants. GbFZ, Gülbahçe fault zone; GhFZ, Güzelhisar fault zone; MeFZ, Menemen fault zone; KFZ, Karşıyaka fault zone; SFZ, Seferihisar fault zone; OFZ, Orhanlı fault zone; İFZ, İzmir fault zone; KFZ, Kemalpaşa fault zone; SdFZ, Spildağı fault zone; MaFZ, Manisa fault zone; UB, Urla Basin; CB, Cumaovası Basin; KMG, Küçük Menderes Graben; KB, Kocaçay Basin; GG, Gediz Graben; MB, Manisa Basin; MP, Menemen Plain.

depressions, namely the outer and the inner bays (Aksu et al., 1987; Sayın et al., 2006). The Outer Bay is oriented NNW–SSE and forms an approximately 20 km wide and 40 km long depression (Fig. 2). The Karaburun Peninsula has a peak altitude of 1200 m (Bozdağ), Foça high is 450 m. Maximum water depth in the Outer Bay is approximately 75 m (Akyarlı et al., 1988; Alpar et al., 1997; Sayın, 2003; Sayın et al., 2006). Based on surface and subsurface morphology, the Outer Bay can be separated into two sub-basins as the Menemen and Gülbahçe sub-basins (Fig. 2; Aksu et al., 1987). The inner and the outer bays are separated by a swell where the water depth decreases down to 13 m. The Inner bay trends E–W and approximately 5–7 km wide and 25 km long (Fig. 2). It is a relatively small and shallow basin having a maximum depth of 20 m, and it is surrounded by the Yamanlar, Seferihisar and Nifdağı highs. The Yamanlar high has a relatively low peak elevation around 110 m while Seferihisar high rises as high as 1000 m from mean sea level. The eastwards on-shore continuation of the inner bay is the alluvial Bornova plain, delimited in the south by the Nifdağı high.

Apart from field-oriented studies, strike-slip activity and recent tectonic activity is also corroborated by earthquake moment tensor solutions of major earthquakes and accumulated GPS data over the last two decades from the region (Kiratzi and Louvari, 2003; Sperner et al., 2003; Zhu et al., 2006; Akyol et al., 2006; Aktuğ and Kılıçoğlu, 2006; Benetatos et al., 2006; Reilinger et al., 2006; Tan et al., 2008; Heidbach et al., 2010). According to Aktuğ and Kılıçoğlu (2006), GPS data obtained around İzmir provides convincing evidence for right lateral strike-slip faulting and a clockwise rotation, related to E–W shortening and N–S extension prevailing in the region. In addition, recent earthquakes around İzmir Bay also provide evidence of distributed strike-slip motion, mainly NE–SW striking right-lateral and NW–SE striking left-lateral (Fig. 2; Kiratzi and Louvari, 2003; Benetatos et al., 2006; Tan et al., 2008; Tan, in press). Ocakoğlu et al. (2005) mapped some of the off-shore active faults around Karaburun Peninsula using seismic reflection data and argued that N–S to NE–SW trending strike-slip faults are responsible for the deformation and current seismicity in the region. Lykousis et al. (1995) have

also reported some Pliocene–Quaternary strike-slip faults around Ikaria and Samos Islands, based on their seismic reflection data.

In this contribution, we provide new structural and kinematic data based on our field studies around İzmir Bay area, which experienced three different phases of deformation since the Miocene. In this context, below we will first describe the general stratigraphy of the Neogene basins in the region. Then, the field data obtained from newly mapped key areas around İzmir Bay will be presented. In the final section, the implications of the presented data will be discussed in the context of the deformation mechanism of the western Anatolian and Aegean region.

2. Methods

In this paper we aimed at better constraining the deformation history around the İzmir Bay area by combining field-based structural analysis and a computer-based palaeostress inversion method using fault slip data. Field-based studies focused on: (i) geological mapping in key areas at a scale of 1/25,000, (ii) identifying stratigraphic units for relative dating of the deformation phases, (iii) collection of kinematic data from the mesoscopic structures for construction of palaeostress configurations. The structural data will be presented using stress and strain terminology (Means, 1976; Twiss and Moores, 1992; Marret and Peacock, 1999), and given in text in the order of: first, general description of a structure and supporting field observations; second, presentation and analysis of structural data; third, interpretation of fault kinematics and deformation phases. Depending on the outcrop availability and density of vegetation/urbanization, we collected fault-slip data systematically along the fault zones wherever possible. On some of the faults, overprinting slickensides indicative of two different faulting episodes or deformation phases were observed and they form the basis for the separation of different deformation phases in the region. Hence, structural observations such as displacement of stratigraphy, style and relative ages of the faults, incompatible shear senses of the cross-cutting faults within the same sampling site, and overprinting/cross-cutting relationships of the features were carefully noted to precisely identify and distinguish the deformation phases. Shear senses along faults were determined by kinematic indicators such as off-set strata, drag of markers, growth fibres in stepped slickensides, crescentic markings, steps and Riedel shear geometry (Means, 1987; Petit, 1987; Hancock and Barka, 1987; Doblas, 1998).

For computer-based inversion of structural data, a number of graphical (e.g. Arthaud, 1969; Alexandrowski, 1986; Krantz, 1988) and numerical palaeostress methods (e.g. Carey and Brunier, 1974; Angelier, 1979, 1984, 1990, 1994; Etchecopar et al., 1981; Armijo et al., 1982; Gephart and Forsyth, 1984; Michael, 1984; Reches, 1987; Marret and Allmendinger, 1990; Will and Powell, 1991; Yin and Ranalli, 1993; Hardcastle and Hills, 1991; Fry, 1999; Yamaji, 2000; Delvaux and Sperner, 2003; Zalohar and Vrabec, 2007) have been developed and most of the software has been made available. Here, however, we used the Direct Inversion Method (INVD) of Angelier (1990), because of its efficiency and robustness in multi-stage deformed areas (Angelier et al., 1981; Kaymakçı et al., 2000, 2003, 2006; Vandycke and Bergerat, 2001; Brahim et al., 2002; Saintot and Angelier, 2002; Sperner et al., 2003; Bergerat et al., 2007; Hippolyte and Mann, 2011). We refer to Angelier (1994) for a detailed review of the method, while for data acquisition/separation techniques we refer to Sperner and Zweigel (2010), and Hippolyte et al. (in press). The INVD technique is based on the reduced stress tensor concept and the estimation of the stress ellipsoid by the shape factor [$\Phi = (\sigma_2 - \sigma_1)/(\sigma_3 - \sigma_1)$] which varies between 0 and 1. Therefore, in areas where the stress ratio approximates 0 or 1, uni-axial stress conditions prevail and faults are not constrained in any direction. Otherwise stress is tri-axial and all of the principal stress magnitudes are significantly different, and the fault orientations tend to develop parallel to σ_2 directions and they approximate to an Andersonian mechanism (Anderson, 1951). During the inversion process, we used the ANG and RUP values (Angelier, 1994) to separate heterogeneous data. The allowable maximum misfit angle (ANG), i.e. maximum misfit angle between observed slip and computed shear stress direction was taken as 25°. The acceptable maximum quality estimator value (RUP), ranging from 0% (calculated shear stress parallel to actual striae with the same sense and maximum shear stress) to 200% (calculated shear stress maximum, parallel to actual striae but opposite in sense) was taken as 50%. Fault slip data exceeding these limits were separated from the data set, and then recomputed as separate tensor.

3. Stratigraphy

The rock units exposed in the İzmir Bay region range from Silurian to Recent. We simplify the tectonic history of the region, and consider the pre-Miocene rocks as basement, only briefly described here. Miocene and younger rocks, however, are described in detail since they are deposited under the influence of relevant tectonic events.

3.1. Basement: pre-Miocene stratigraphy

The basement considered here consists of four units (Fig. 3), the Menderes Metamorphic Core Complex, the Cycladic Metamorphic Core Complex, the Paleozoic to Mesozoic rocks of the Karaburun Belt, and the Bornova Flysch Zone.

The Menderes Metamorphic Core Complex, also known as Menderes Massif, is one of the largest metamorphic series in the Alpine–Himalayan chain and is derived from metamorphism related to late Proterozoic to early Paleozoic Pan-African orogenic events as well as to Mesozoic to Cenozoic Alpine events (Bozkurt and Park, 1997; Okay, 2001; Candan et al., 2001; Özer et al., 2001; Lips et al., 2001; Özer and Sözbilir, 2003; van Hinsbergen, 2010). It is delimited in the west by the İBTZ (Figs. 1 and 2) and is exhumed by low-angle normal faults, which uplifted and exposed medium to high-grade metamorphic rocks and separated the metamorphic core from the unmetamorphosed to lower grade metamorphic cover series. These low angle detachment faults are dissected by high angle normal faults that control mainly the northern and southern margins of major E–W trending basins in western Anatolia, such as the Gediz and Büyük Menderes basins (Koçyiğit et al., 1999; Sözbilir, 2001; Bozkurt and Sözbilir, 2004).

The Cycladic Metamorphic Core Complex is an Eocene high-pressure metamorphic belt exposed mainly at the southern margin of Kocaçay Basin in western Turkey (Fig. 2). It extends westwards and is exposed on some Greek Islands, within a crescent shape belt extending from Turkey to the southernmost part of mainland Greece (Figs. 1 and 2). It consists primarily of large marble bodies embedded in schists. In the Kocadağ High, it comprises mica- and calc-schists, marbles, meta-cherts, serpentines and meta-volcanic rocks (Fig. 2; Okay, 2001; Sözbilir et al., 2011).

The Karaburun Belt comprises rock units extending from the Paleozoic to the late Cretaceous related to the opening and closure of the Tethyan Ocean (Erdoğan, 1990; Kozur, 1997; Robertson and Pickett, 2000; Tatar-Ekrül et al., 2008). It has a wide range of rock types, encompassing granites to turbiditic sequences with olistholites and tectonic blocks ('wild flysch') with ages ranging from Paleozoic to Cretaceous and belonging to different tectonic

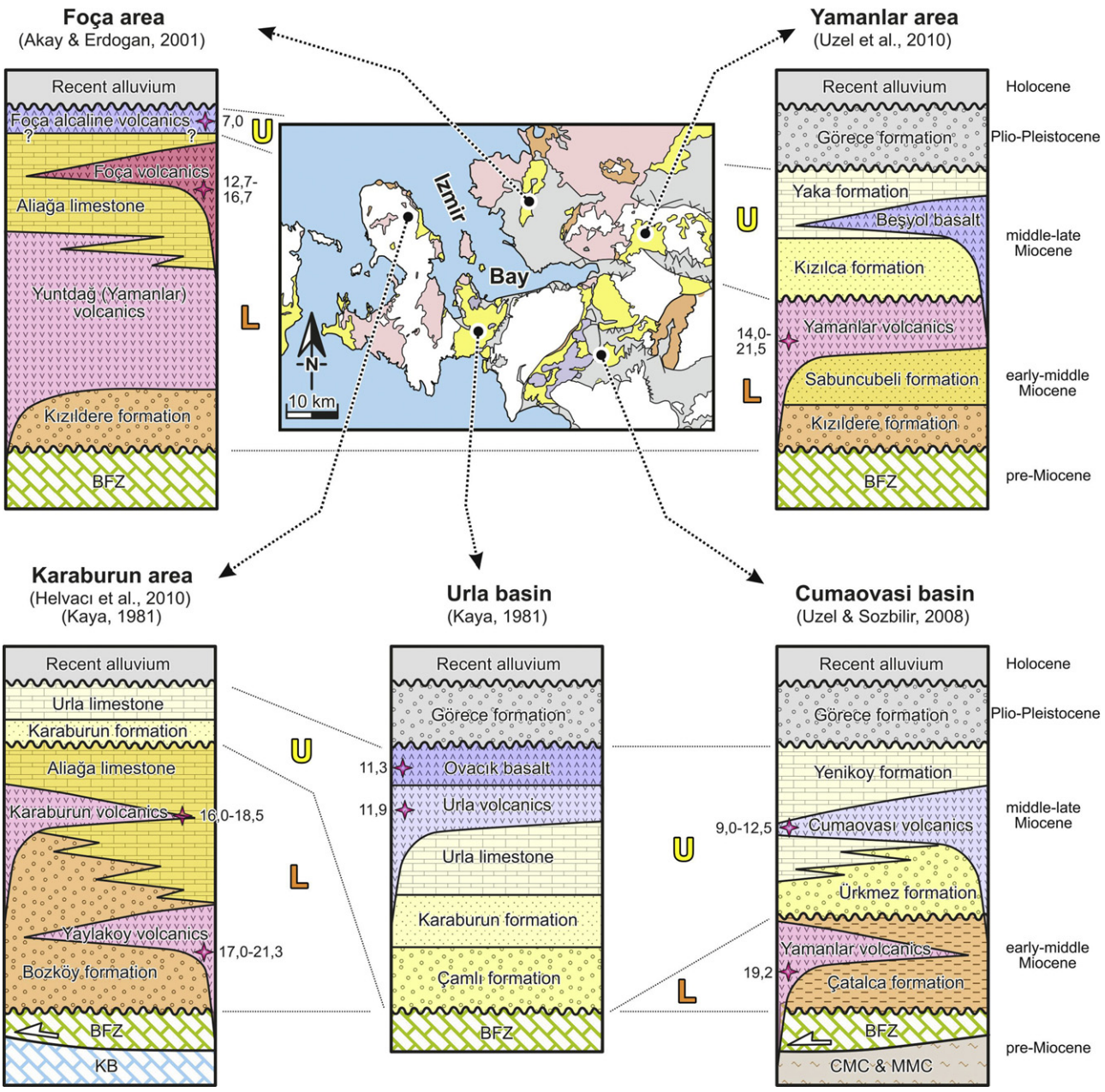

Fig. 3. Generalized stratigraphy of Miocene basins around İzmir Bay. U (L), Upper (Lower) sequence of Miocene deposits; BFZ, Bornova Flysch Zone; KB, Karaburun Belt; CMC, Cycladic Metamorphic core Complex; MMC, Menderes Metamorphic core Complex. See text for references on radiometric ages, indicated by purple stars.

settings and depositional environments (see Erdoğan, 1990; Kozur, 1997; Çakmakoğlu and Bilgin, 2006 for detail).

The Bornova Flysch Zone, also known as Bornova Mélange (Erdoğan, 1990), is defined as a tectonic belt on the northwestern margin of the Anatolide-Tauride Block (Okay and Altıner, 2007; Okay et al., in press). It is a 60–90 km wide and approximately 230 km long, NE-trending tectonic zone lying between the Menderes Metamorphic Core Complex and the Karaburun Belt (Fig. 1). It is well exposed in the Seferihisar and Nifdağı highs along the southern margin of the Inner of İzmir Bay (Fig. 2). The Bornova Flysch Zone is composed of an extremely deformed and locally metamorphosed flysch-like sedimentary matrix of Maastrichtian–Paleocene age, with blocks of Mesozoic limestones, serpentinites and submarine mafic volcanic rocks (Erdoğan, 1990; Sarı, in press; Okay et al., in press).

3.2. Miocene stratigraphy

The Miocene stratigraphic record of the İzmir Bay area is characterized by two main volcano-sedimentary successions separated by an angular unconformity: (i) lower sequence, and (ii) upper sequence. Here, we focus on the main geometry and characteristics of these successions within five areas: Karaburun, Urla, Cumaovası, Yamanlar and Foça (Fig. 3).

Karaburun area: The Miocene volcano-sedimentary units of Karaburun area begin with a base member of the lower sequence, the Bozköy Formation (Helvacı et al., 2009). It crops out mainly in the northwestern part of the area, in the vicinity of Salman village, where the formation consists of reddish- to grayish-brown conglomerate, gray sandstone and greenish-gray mudstone alternations, resting with an erosional surface on the rocks of the Karaburun Belt. Around the north of Sarpıncık village, the Bozköy

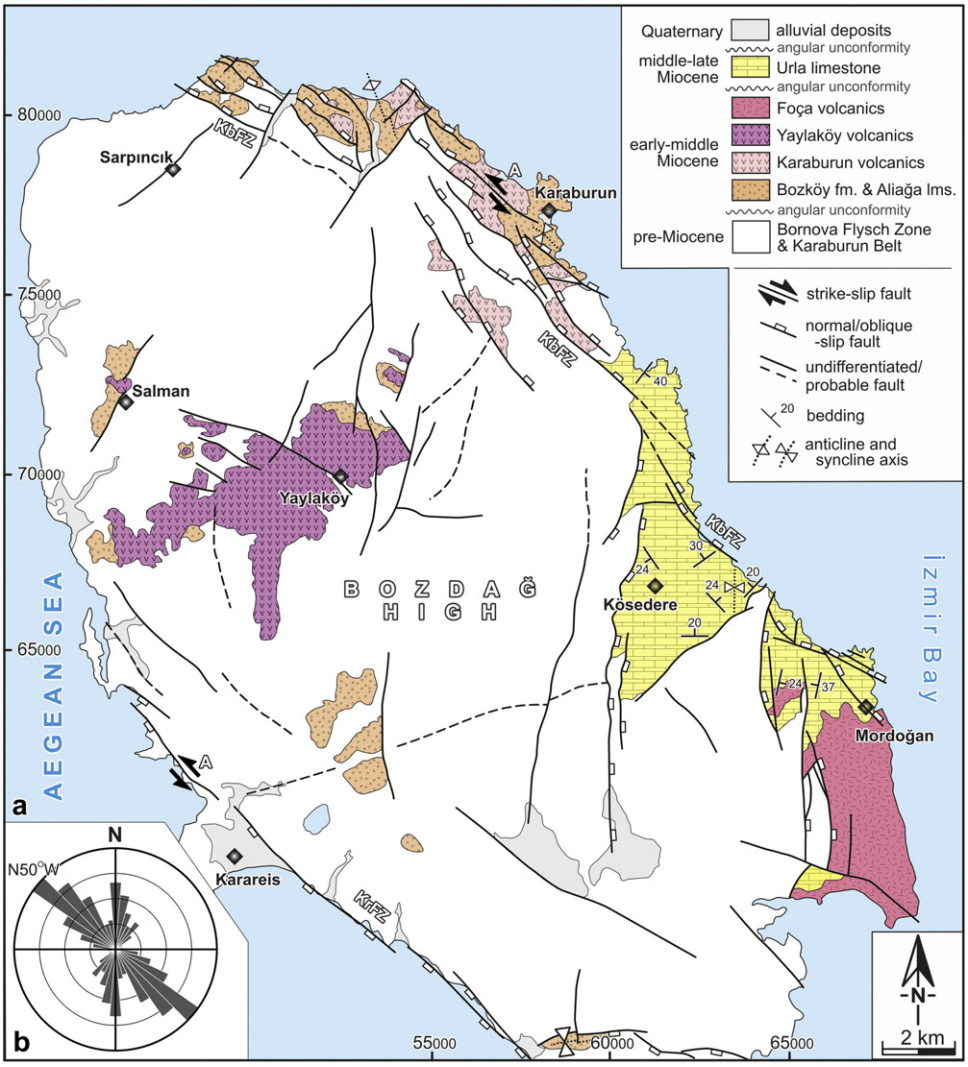

Fig. 4. (a) Detailed geological map of Karaburun area (compiled from Tatar-Ekrül et al., 2008; Helvacı et al., 2009, and this study). A refers to older than Miocene strike-slip faulting along the Karaburun and Karareis fault zones. See Fig. 2 for location. (b) Length weighted rose diagram of the strikes of all faults in the area. Note that two directions, N50°W and N–S, dominate in the region.

Formation laterally and vertically passes into an alternation of white to brown lacustrine limestone and claystone (Aliağa limestone of Kaya, 1981). During the deposition of the Aliağa limestone in the latest early Miocene, several volcanic units are emplaced. The first products of this volcanic activity around the Karaburun area are known as Yaylaköy volcanics and are composed of lava flows and associated pyroclastic rocks with a basaltic–andesitic composition dated as 21.0–17.3 Ma (Borsi et al., 1972; Helvacı et al., 2009). Higher in the section, Karaburun volcanics aged 18.5–16.0 Ma and Foça volcanics (aged 16.7–12.7 Ma in the Foça area; Fig. 3) are emplaced during the deposition of the Aliağa limestone (Figs. 3 and 4; Kaya, 1981; Helvacı et al., 2009).

The Urla limestone in the Karaburun district characterizes the upper sequence of the Miocene volcano-sedimentary unit. It is composed mainly of yellowish white, thick-bedded limestone and brownish-gray to white mudstone, greenish-gray claystone alternations and gray sandstone interlayers.

Urla basin: East of the Karaburun Peninsula is the Urla Basin, where only middle to late Miocene strata are exposed (Fig. 3; Savaşçın, 1978; Kaya, 1979, 1981; Sümer, 2007). The base of the Urla Basin is the Çamlı Formation and it includes reddish- to brownish-gray, semi-consolidated conglomerates, alternations of sandstone and mudstone, with limestone interlayers. Higher in the sequence, these conglomerates pass into sandstones and mudstones (Karaburun formation). The Urla limestone conformably overlies the other clastic units of the basin, and represents the higher part of the upper sequence.

In the central part of the basin, the volcanic units are exposed as the Urla volcanics and the Ovacık basalt (Kaya, 1981; Helvacı et al., 2009). The Urla volcanics are mainly composed of rhyolitic lava flows, porphyritic domes and dykes. These lava flows yield a (K/Ar) age of 11.9 Ma (Borsi et al., 1972). The overlying Ovacık basalt is dated (K/Ar) at 11.3 Ma by Borsi et al. (1972).

Cumaovası basin: The Cumaovası basin is located within a topographic depression between the Seferihisar and Nifdağı highs and comprises five major lithostratigraphic units, from base to top: Çatalca Formation and Yamanlar volcanics as the lower sequence; Ürkmez Formation, Yeniköy Formation and Cumaovası volcanics as the upper sequence (Genç et al., 2001; Uzel and Sözbilir, 2008). In the lower sequence, the Çatalca Formation is composed of thinly-to-thick bedded conglomerates, sandstones, siltstones and shale alternations including coal seams of early-middle Miocene age (Akartuna, 1962; Kaya, 1979, 1981; Genç et al., 2001; Sözbilir et al., 2004). The overlying Yamanlar volcanics are made up of

calcalkaline volcanic rocks that are exposed in the northern rim of the Cumaovası basin. In this locality, the unit is dated (K/Ar) as 19.2 Ma by Borsi et al. (1972).

The upper sequence in the Cumaovası Basin starts with the Ürkmez Formation (Eşder and Şimşek, 1975; Genç et al., 2001; Uzel and Sözbilir, 2008), which is dominated by reddish-brown conglomerates and sandstones interfingering with brownish-gray lacustrine limestone lenses. Upwards, the dominant lithology is a fining-upward sequence of mudstones that gradually grades into yellowish, thinly- to medium-bedded lacustrine limestones and green laminated claystone alternations (Yeniköy Formation). Laterally, the unit interlayers with pyroclastic layers of the Cumaovası volcanics. These are primarily composed of rhyolitic pyroclastic rocks and lava flows, occasionally with obsidian and perlites (Eşder and Şimşek, 1975; Özgenç, 1978; Genç et al., 2001; Uzel and Sözbilir, 2008). The outcrops of the unit are generally aligned in a NNE–SSW direction, close to the volcanic centers in the basin. The (K/Ar) ages of the Cumaovası volcanics range 12.5–9.0 Ma (Borsi et al., 1972; Özgenç, 1978; Genç et al., 2001).

Yamanlar area: The lower sequence is well exposed within and beyond the northern margin of the Inner Bay of İzmir (Fig. 3). It consists of two sedimentary units namely the Kızıldere and Sabuncubeli Formations overlain by the Yamanlar volcanics. The sedimentary units consist primarily of conglomerates at the base and grade upwards into sandstone-shale alternations (Kızıldere Formation). Upward in the stratigraphy, mudstones and then limestones become dominant (Sabuncubeli Formation). Subsequently, the sedimentary rocks pass into volcanic rocks named as Yamanlar volcanics. These are generally calcalkaline in nature and are composed of several lava flows, layers of pyroclastic rocks, dykes and domes of dacitic, andesitic, rhyolitic and basaltic compositions. Based on K–Ar dating the age of the unit is 14.0–21.5 Ma, which corresponds to early-middle Miocene (Borsi et al., 1972; Savaşçın, 1978; Ercan et al., 1996).

The upper sequence around Yamanlar area is a middle to late Miocene volcano-sedimentary succession, well exposed along the İzmir and Manisa highway near Menemen (Akartuna, 1962; Akdeniz et al., 1986; Uzel et al., 2012). It rests unconformably on the Yamanlar volcanics, starting with the slightly deformed, folded and faulted Kızılca formation composed of continental clastic rocks, intercalated with lacustrine carbonate levels. The sequence passes upward into grayish-brown sandstones and green mudstones, while it ends with light-gray and yellowish-white lacustrine limestones at the top, the Yaka formation (Akdeniz et al., 1986; Uzel et al., 2012). At the transitional contact between these two sedimentary units, laterally discontinuous basaltic lava is emplaced, the Beşyol basalt: dark-brownish olivine basaltic lavas showing peperitic texture at the contact with the sedimentary rocks. There is no published radiometric age for these basaltic units, but the age of the Beşyol basalt can be taken as late Miocene based on superposition.

Foça area: A thick volcanic succession of andesitic to rhyolitic lavas and sedimentary rocks characterizes the lower sequence in the Foça area north of İzmir Bay (Foça volcanic complex of Akay and Erdoğan, 2004) (Fig. 3). The Yuntdağ volcanics are composed mainly of andesitic and trachy-andesitic lava flows, domes and dykes, with coarse-grained to blocky pyroclastic flow deposits. Reddish-black coloured porphyritic andesites, black aphanitic andesites, flow breccias and perlites are also common in this unit. The age of the Yuntdağ volcanics is of 14.0–21.5 Ma (Borsi et al., 1972; Savaşçın, 1978; Innocenti et al., 1982; Ercan et al., 1985). The unit grades laterally into, and is overlain by the Foça volcanics (Akay and Erdoğan, 2004), which comprises mainly rhyolitic pyroclastic rocks and small rhyolitic domes, dykes and lava flows. The upper part of the unit includes mafic alkaline lavas and distinctively NE–SW-oriented dykes. Ages of the Foça volcanics range 12.7–16.7 Ma (Savaşçın, 1978; Ercan et al., 1985 and references therein). The conformably and gradationally overlying Aliağa limestone is composed primarily of yellowish-white-coloured, medium- to thick-bedded, gastropod-rich lacustrine limestones with brownish-yellow clayey limestone and greenish-brown mudstone interbeds (Kaya, 1981; Akay and Erdoğan, 2004).

3.3. Post-Miocene stratigraphy

The post-Miocene continental and shallow marine deposits unconformably overlie the Miocene volcano-sedimentary successions. These are the Plio–Pleistocene Görece Formation, and Holocene alluvial and shallow marine deposits (Figs. 2 and 3). The Görece Formation is composed mainly of reddish-brown, semi-consolidated, continental clastics composed of reddish-brown sandstone and conglomerate alterations. It rests on an erosional surface of the Miocene sequence with a basal conglomerate. According to Uzel and Sözbilir (2008) it is deposited in an alluvial fan environment and it can be correlated with the Plio–Pleistocene Sütçüler Formation exposed in the Gediz graben (Sarıca, 2000; Sözbilir et al., 2011). Holocene alluvial deposits are characterized by alluvial fan deposits that are interfingering with alluvial plain deposits along the streams, and with fan-delta to shallow marine deposits along the shoreline of İzmir Bay.

4. Late Cenozoic structures

In terms of structures, the first key area we describe is the Karaburun area, located in the northern side of Karaburun Peninsula and covers some 60 km^2. The second key area is the Menemen area, located at the western margin of Yamanlar high and approximately 120 km^2. The third one is the Yaka area lying between the Yamanlar and Spildağı highs, and covers some 150 km^2. All key areas are denoted in Fig. 2, referring to Figs. 4, 7 and 10 respectively.

4.1. Karaburun area

The main late Cenozoic structures mapped around the Karaburun area consist of the Karaburun and Karareis fault zones, NNE-striking conjugate faults and a number of folds (Fig. 4).

Karaburun fault zone (*KbFZ*): It is a 2–4 km wide, 25 km long, approximately N50°W-striking and NE-dipping fault zone comprising several synthetic faults that display a well-developed step-like morphology with concave/curvilinear range-front. It controls the SW margin of the İzmir Bay at the NE side of the Bozdağ high (Figs. 2 and 4a). The fault zone starts north of Mordoğan village and runs in a N50°W trend to the Karaburun village, where it bents west to N65°W and bends again to N50°W. Further north, it jumps two times to southwest juxtaposing conjugate faults, and then disappears under the water of the Aegean Sea in a N70°W trend north of Sarpıncık village (Fig. 4a). NW of Karaburun village, a couple of relatively small SW dipping antithetic faults are also recognized (Figs. 4 and 5a).

Along the KbFZ, we collected more than 90 fault plane data to establish its kinematic behaviour (plots 1A, 2, 3 and 4A in Fig. 6). The observed slicken-lines along the KbFZ are between 45° and 88°. Depending on the direction of the fault plane and the position of the measurement site along the fault zone, the amount of the obliqueness of the slip vectors and also the orientation of the calculated stress axes (see Palaeostress section) show some kinematic variation along fault from one tip to the other, in accordance with the nature of faulting (Maniatis and Hampel, 2008). The dip angles of the fault planes are ranging between 50° and 88°, but most of them are more than 75°, surprisingly steep for a normal fault. According to field observations, the general structural style of the KbFZ is

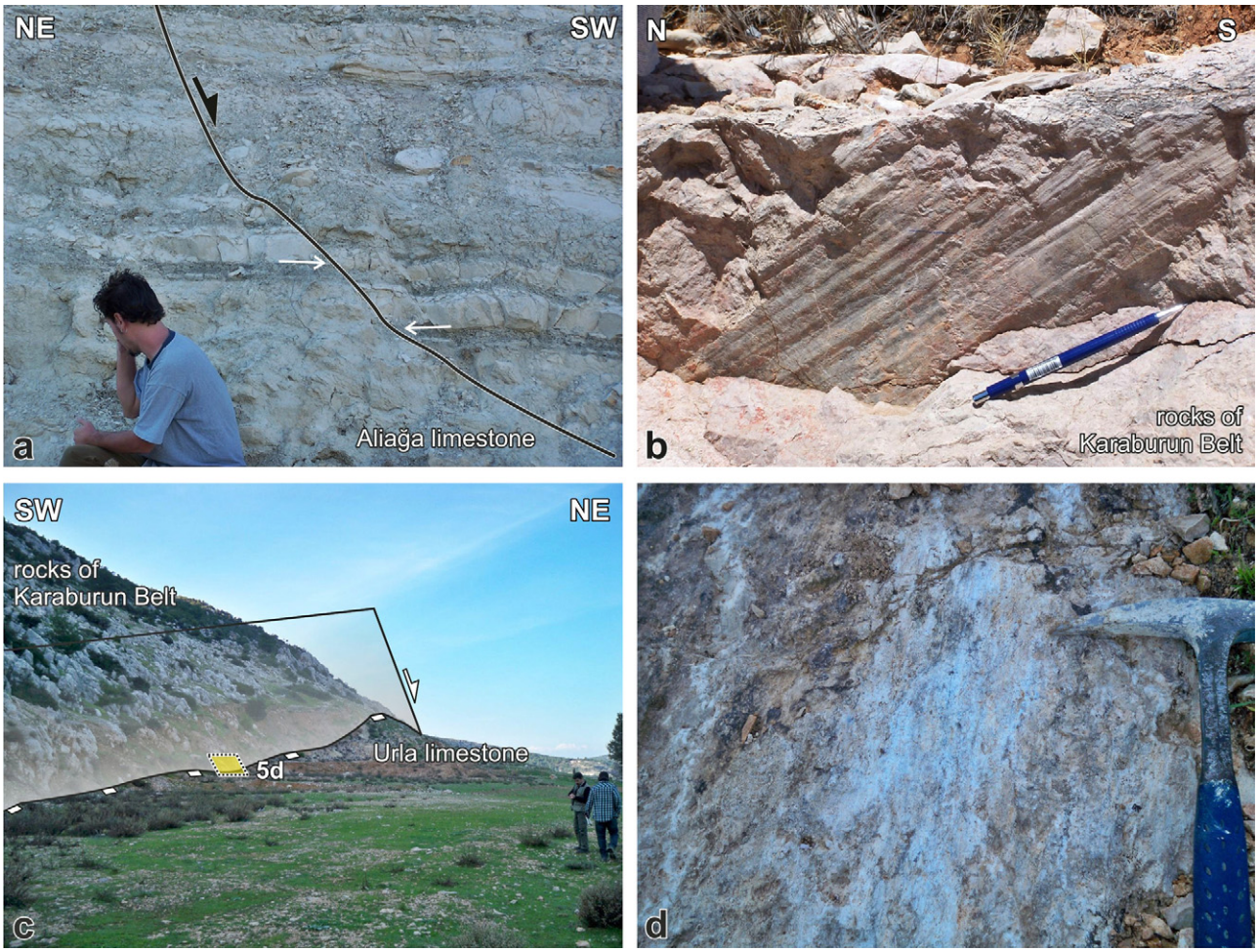

Fig. 5. Field photos of post-Miocene structures from the Yaka area. (a) A secondary antithetic normal fault parallel to the Karaburun fault zone, W of Karaburun village. (b) Close-up view of older strike-slip faulting along the Karaburun fault zone, SW of Karaburun village. (c) A distinct NNE-striking fault trace west of Kösedere village. (d) Close up view of a normal fault plane with well-preserved slickenlines.

identified as an oblique-slip normal fault with an average rake of 60°W, trending in N50°W direction.

Along the KbFZ, we also document evidence of an older strike-slip faulting with 37 fault slip data, from several locations along the fault zone. The computed data is presented (in Fig. 6) as projections in 1B and 4B. The observed older slicken-side set has a left-lateral strike-slip character represented by slickenlines with an average rake of 20 W, and consistently overprinted by younger slickensides having an oblique-slip normal character. Therefore, we suggest that the KbFZ formerly had a strike-slip motion, and has afterwards been reactivated as an oblique-slip normal fault zone. The younger oblique-slip faulting is also documented by seismic events near the KbFZ in outer bay (Fig. 2). The KbFZ has cut and displaced the basement rocks of the Karaburun Belt, Bornova Flysch Zone, and the Miocene volcano-sedimentary strata.

Karareis fault zone (*KrFZ*): The NW-striking KrFZ cuts and displaces the rocks of the Karaburun Belt along the SW margin of Bozdağ High where it delimits the western side of Karaburun Peninsula (Figs. 2 and 4). The zone is 1–3 km wide, 20 km long, and is approximately parallel to the KbFZ on the other side of the Bozdağ high (Fig. 4a). The KrFZ also includes several link and antithetic faults with steeply dipping planes. We collected 34 fault plane data along the fault zone. According to computed data, the major strike is around N50°W and the main dip is approximately 75°SW (plots 6, 7A, 7B, and 8 in Fig. 6). Observed slickenlines range 64–80°, characterizing the oblique-slip normal fault character of the KrFZ. Like the KbFZ, the KrFZ also bears obvious evidence of early left-lateral strike-slip motion: overprinting kinematic indicators show reactivation of the KrFZ as an oblique-slip normal fault zone (plot 7A in Fig. 6). On the basis of 8 fault plane data from different locations around Karareis village, the older striation has an average rake of 11°E, whereas the younger ones are around 70°W. Seismicity of the northern Karaburun Peninsula also provides evidence that dip-slip faulting is younger than strike-slip, in good agreement with the field evidence (Fig. 2).

NNE-striking faults: These faults are predominantly observed around the N and NE sides of the Bozdağ High (Fig. 4a). More than 50 fault plane measurements along the NNE-striking faults show that they are generally steeply dipping (around 70°) and have mainly a strike-slip character (Fig. 6). As an example, N of Sarpıncık where the Miocene strata are cut and deformed by a series of left-lateral NE-trending strike-slip faults (Fig. 5b), kinematic data show left-lateral strike-slip faulting with a minor normal component as indicated by sub-horizontal rakes (15–25°SW) (plot 9B on Fig. 6). The average dip of the fault planes is approximately 80° to NW.

West of Kösedere village, four obvious NNE-striking structural lineaments are mapped, where the limestones of the Karaburun Belt are juxtaposed with Miocene carbonates and clastics of the Urla Formation (Figs. 4a, 5c and d). These structures display a typical step-like normal-fault morphology stepping down eastwards. Along these, we collected 14 fault plane data to understand the nature of faulting. Some of the fault planes have locally

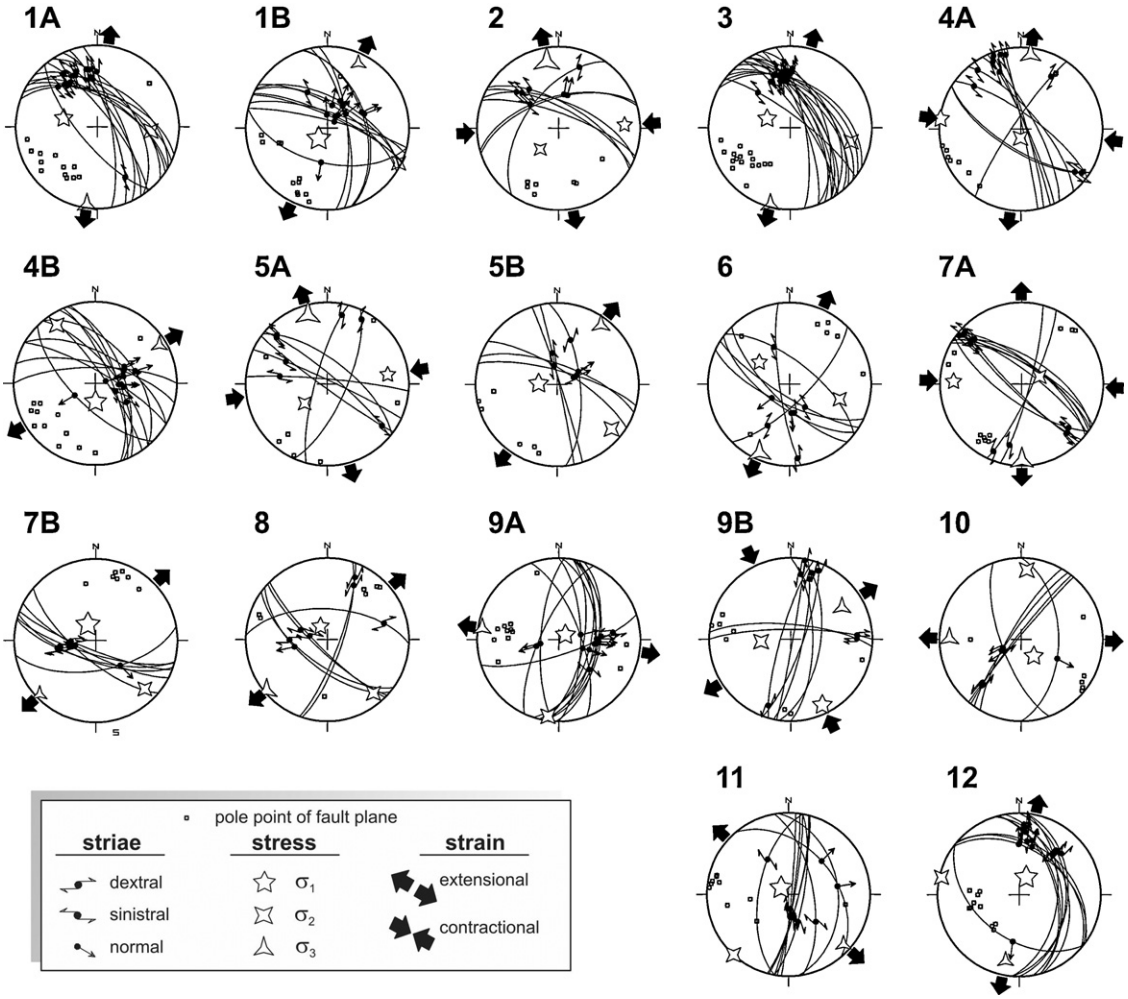

Fig. 6. Lower-hemisphere equal-area projection of fault planes, slickenlines, and constructed palaeostress configurations for the Karaburun area. Numbers refer to the localities as depicted in Fig. 14a.

preserved slickensided surfaces showing normal slip (>60°), on average dipping 60°E (plot 12 in Fig. 6). West of Mordoğan, another NNE-trending fault set was mapped and archived with 14 fault plane data. It delimits the eastern part of the Bozdağ High, cuts and displaces volcanoclastics of the Foça Formation and lacustrine sediments of the Urla Formation (Fig. 4a) with several subparallel faults having an average dip of 55°E. Well-exposed slickenlines on these planes show normal fault activity with a minor left-lateral strike-slip component as indicated by sub-vertical rakes (50–85°N) (plot 11 in Fig. 6). The NNE-striking faults observed around Kösedere and Mordoğan villages have cross-cutting relationships with the fault sets of the KbFZ (Fig. 4a).

Additionally, along the one NE-striking fault located at 2 km NE of Sarpıncık village, we collected 13 overprinted slickenside data supporting the evidence for two different styles of faulting. Here, the red clastic part of the Miocene strata (Bozköy Formation) is cut and offset by high-angle fault planes dipping NW and shows a well-preserved overprinting expressed as two sets of slickensides. The early set has average rakes of 80°S while the younger set has average rakes of 25°S (projections 9A and 9B, respectively). Likewise, the other NNE-striking faults observed around Sarpıncık and Karaburun villages also have cross-cutting relationships with the faults of the KbFZ.

Folds: A series of anticlines and synclines were mapped in the Karaburun distinct. The average lengths of these folds are not more than 2 km. They are developed mainly in the lower sequence of Miocene strata around Karaburun town and at the southernmost part of Karaburun Peninsula (Fig. 4a). They are relatively small, open to gently plunging folds. Except east of Kösedere village, their axes are mostly parallel to the nearby normal faults, which indicates that they are forced (drag) folds developed on top of rotating fault blocks along horizontal axes (i.e. cover deformation).

4.2. Menemen area

In this area, three different fault and fold sets that are related to deformation of the Miocene units have been recognized during field studies. These structures include NE-striking strike-slip faults (Harmandalı fault zone), approximately E–W striking oblique-slip faults, NW-striking strike slip faults, and NNE-trending folds (Fig. 7). Apart from that, part of a regional NE–SW-trending strike-slip fault system, which we named the Harmandalı fault zone and which delimits the Yamanlar high to the west, is documented here for the first time together with its kinematic characteristics.

Harmandalı fault zone (*HFZ*): It runs along the western scarps of the Yamanlar High and can be traced for approximately 15 km between İzmir Bay and Menemen town (Fig. 7a). The fault zone comprises several relatively small-scale faults striking mainly in a NE–SW-direction. The Yamanlar volcanics, the Kızıldere Formation and the rocks of Bornova Flysch Zone are tectonically juxtaposed along the fault zone (Figs. 7a and 8a). We measured 69 fault planes

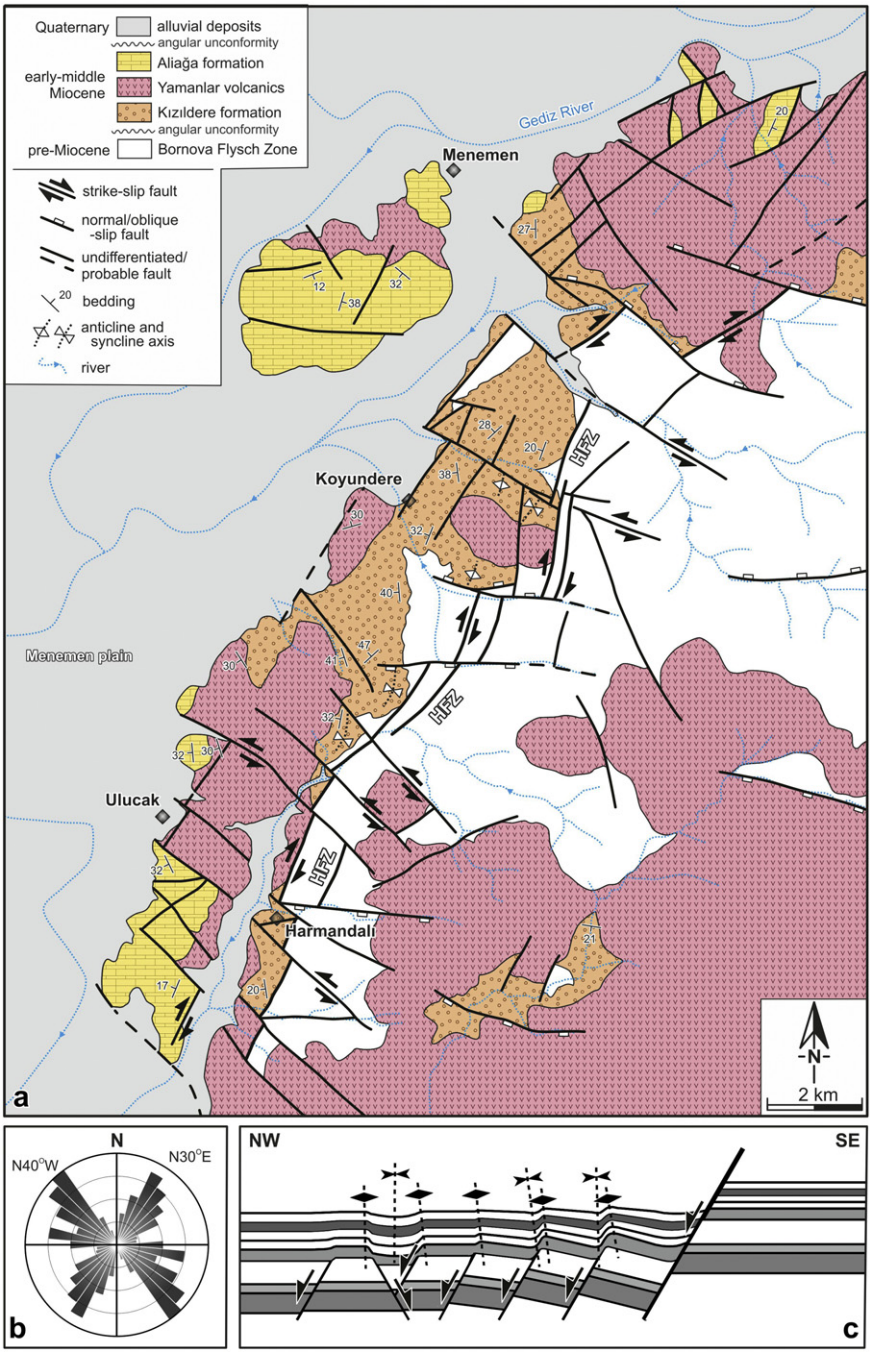

Fig. 7. (a) Detailed geological map of the Menemen area (see Fig. 2 for location), and (b) rose diagram of faults in the area. Note the two dominant directions of N40°W and N30°E. (c) Drag fold mechanism, developed on the cover of rotating fault blocks in the area.

along the HFZ, projected as plots of 13, 14, 16, and 18 (Fig. 9). According to kinematic data, the main motion on the fault surfaces is right-lateral strike-slip with an average rake of 20° (Fig. 8b). Here, the fault planes have an overall strike of between N5°E and N65°E (Figs. 7b and 9), and dip of approximately 75° to the NW. The HFZ is systematically cut and displaced by E–W-trending faults (Fig. 7a). According to the regional picture of the main faults, the distinct NE trending HFZ controls the Menemen plain and it seems that this zone was extending to the south of İzmir Bay into the Seferihisar fault zone. Later, it was dissected by E–W faults that control the northern (Karşıyaka fault zone) and southern margin (İzmir fault zone) of the inner İzmir Bay. The Seferihisar fault zone bends and merges clearly with the İzmir fault zone, but the younger evidence about the joining of Harmandalı fault zone and Karşıyaka fault zone is mostly under the alluvium because of the rapid sedimentation in the Menemen plain (Fig. 2).

E–W-trending faults: These faults are developed all along the HFZ, the western margin of Yamanlar high (Fig. 7a). Several well-exposed fault planes strike approximately E–W (Fig. 7b), with an average dip of 65° both N and S (Fig. 8c). Based on 22 fault plane data, well-preserved slickenlines on these planes show oblique-slip motion with right-lateral component as indicated by rakes ranging between 22° and 70° (plots 15 and 17 in Fig. 9). In map view, the E–W-trending faults cut and displace some faults belonging to the HFZ, and are in turn displaced by NW-trending faults around Harmandalı village (Fig. 7).

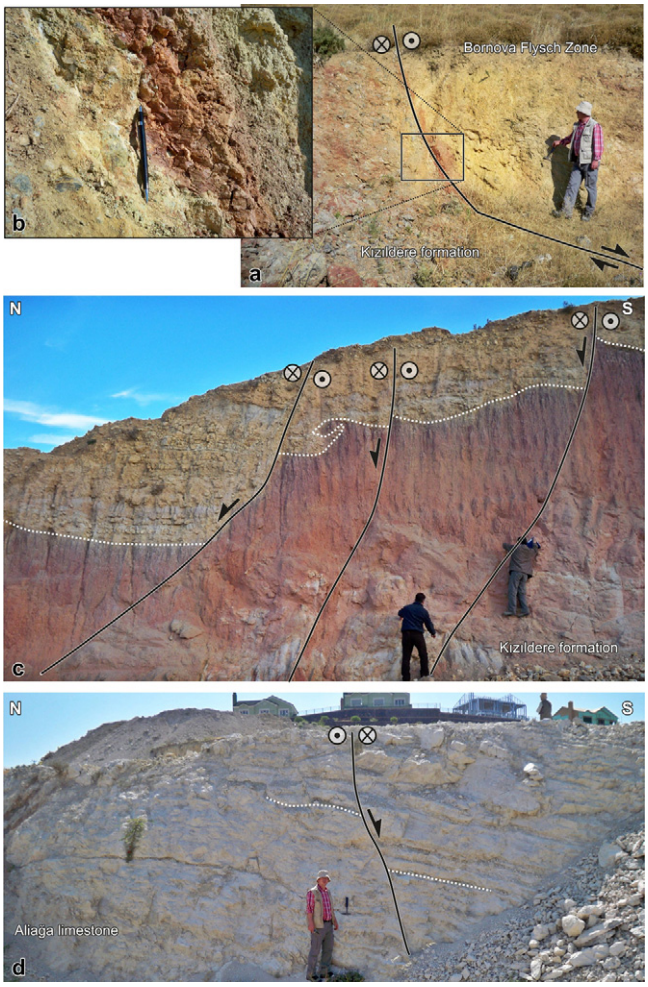

Fig. 8. Field photos of post-Miocene structures from Menemen area. (a) The reddish sandstone and conglomerate alternation of the Kızıldere formation juxtaposed with intensely deformed sandstones of Bornova Flysch Zone along the Harmandalı fault zone. (b) Close up view of slickenside surfaces. (c) Well-exposed fault planes of E–W striking faults. Oblique-slip offset of the Kızıldere formation is very obvious. (d) A field photo of NW striking strike-slip fault with minor normal-slip component.

NW-trending faults: The mapped NW–SE oriented faults are apparently the youngest structures in the area. These were clearly expressed by the linear NW-trending topographic valleys in the morphology (Fig. 7). The observed fault planes show that the main motion along these faults is left-lateral strike-slip with a minor normal component (Fig. 8d). The fault planes are well preserved, striking N30–50°W (Fig. 7b) with an average dip of 80°SW and NE, and the observed striations having rakes less than 20° (plot 18 in Fig. 9). In particular, NE of Koyundere, a series of NW-trending strike-slip faults cut and displaced the Miocene strata, but no Quaternary activity of these faults could be observed because of being mostly concealed by alluvial deposits.

Folds: Several mesoscopic anticlines and synclines trending in a NNE-direction are observed in the Menemen area (Fig. 7a). They have occurred mainly in the Kızıldere Formation and are mostly sub-parallel to the Harmandalı fault zone and are almost always parallel to the nearby oblique faults. They are mostly open and gently plunging southwest to northeast. From the Yamanlar High westwards towards the basin center, these folds are getting more open and disappear in the younger beds. Based on these relationships we propose that these faults are drag folds developed on the hanging-wall block of normal fault blocks (Fig. 7c).

4.3. Yaka area

The area lying between the Yamanlar and Spildağı highs along the northern margin of the inner bay of İzmir is mainly shaped by strike-slip faults, namely of the Karaçay, Gürle, Manisa, Kemalpaşa and Spildağı fault zones (Figs. 2 and 10a). Özkaymak and Sözbilir (2008), and Sözbilir et al. (2011) previously documented some of these structures, especially the normal faults along the margin of the Manisa Basin and along the western rim of the Gediz graben, respectively. In particular, the field observations on the Manisa and Karaçay fault zones by Özkaymak and Sözbilir (2008) support reactivation on NE-trending faults. Here, we provide additional field data and kinematic analyses on their continuation in the Yaka Area, to shed more light on the structural link between NE–SW and E–W striking fault systems—it plays a key role in understanding the kinematic relationship between strike-slip and normal faults in western Anatolian extensional tectonics. Additionally, in the Yaka area two distinct fold patterns, trending N–S and E–W, within the Miocene strata are recognized and mapped during field studies.

Karaçay fault zone (*KçFZ*): This is a 2 km wide and 15 km long NE-striking fault zone tracing between the Yamanlar and Spildağı highs (Figs. 2 and 10a). It cuts and deforms the Bornova Flysch Zone, and the Miocene volcano-sedimentary strata. We collect 59 fault plane data along the KçFZ, and present them as plots 19A, 19B, 20A, and 20B in Fig. 11. The fault zone includes strike-slip faults, which were formed by a principal displacement zone

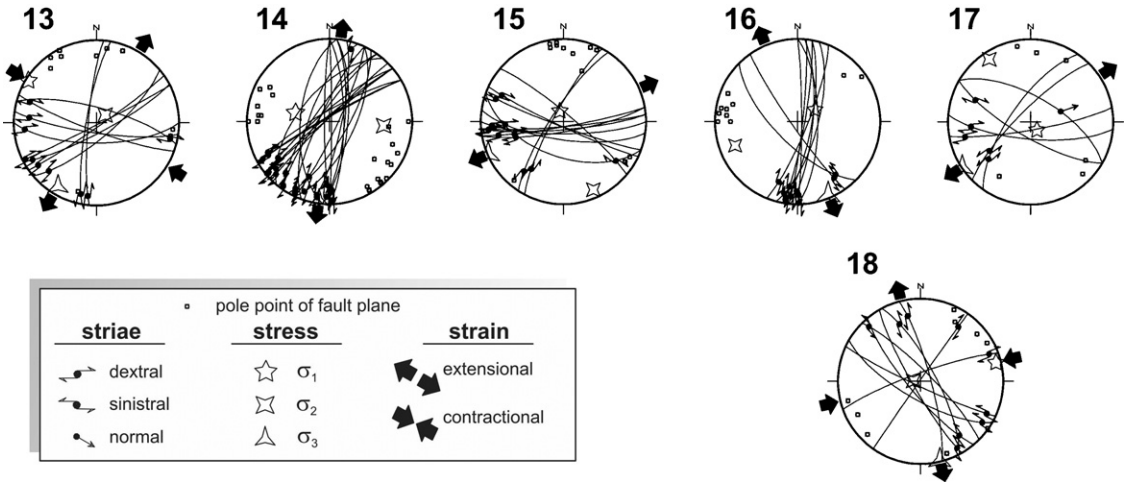

Fig. 9. Lower-hemisphere equal-area projection of fault planes, slickenlines, and constructed palaeostress configurations for the Menemen area.

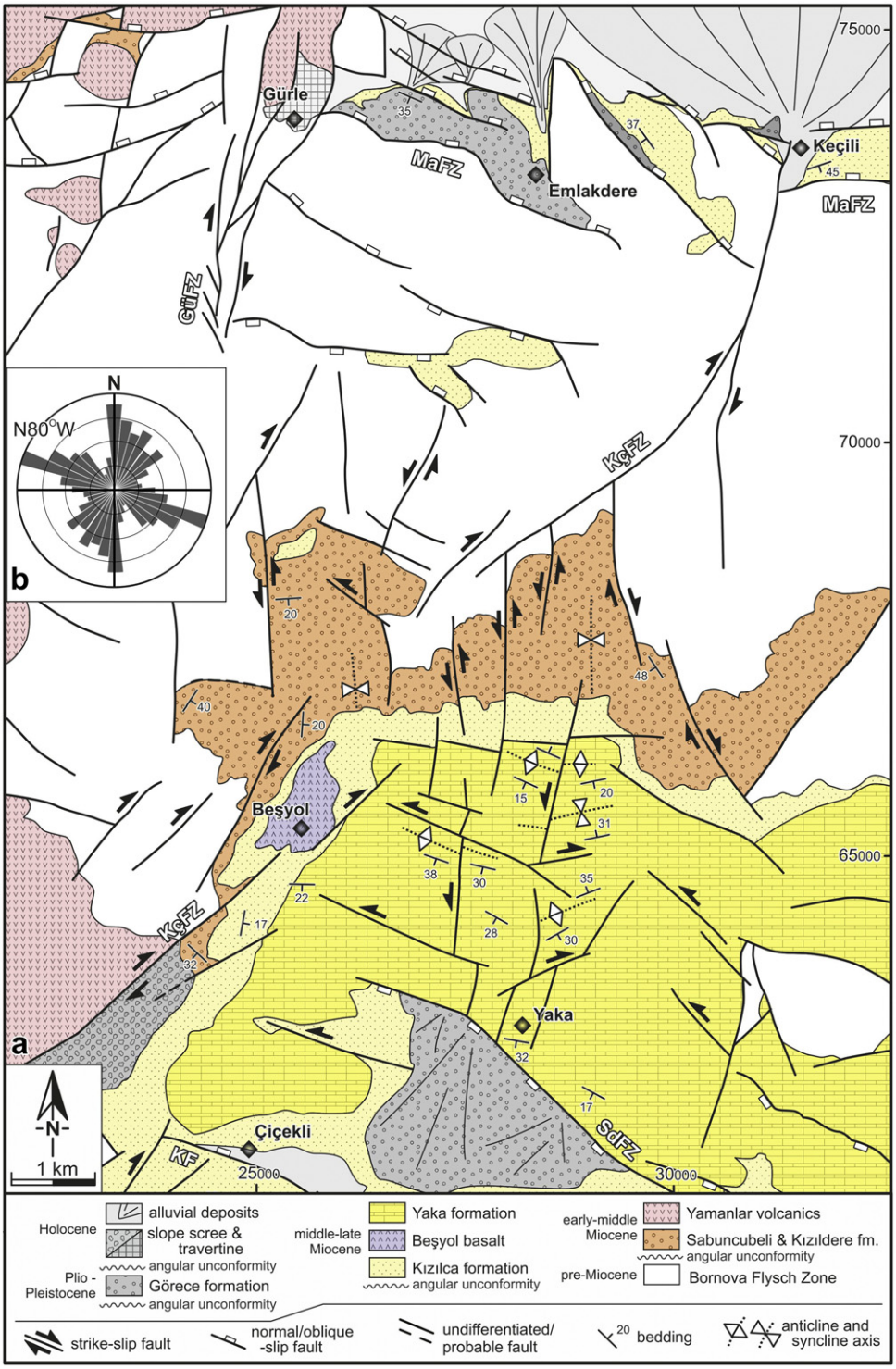

Fig. 10. Detailed geological map of the Yaka area (northern side of the mapped area is compiled from Özkaymak and Sözbilir, 2008; southern side is from this study). See Fig. 2 for location.

striking between N05–40°E, and Riedel faults striking between N–S and N45°W (Fig. 10b). Most of these faults are generally dipping more than 70° to the S, and are clearly traced by well-developed fracture zones generally having widths of >10 m (Fig. 12b).

NE of Beşyol and NW of Çiçekli villages, the existence of an early left-lateral strike-slip faulting were documented with 24 fault plane data (plots 19A and 20A). Here, the earlier left-lateral slip lines with rakes ranging 04–20°N have been overprinted by a series of younger right-lateral strike-slip striations with an average rake of 20°S. The measured fault planes have strikes around N35–40°E with an average dip of 85° to the SE. Near Keçili village, reactivation along the KçFZ was also mentioned with kinematic data by Özkaymak and Sözbilir (2008). In map view, the KçFZ shows cross-cutting relationships with the E–W-trending normal faults such as the Manisa, Kemalpaşa and Spildağı fault zones (Figs. 2 and 10a).

Kemalpaşa (*KFZ*) *and Spildağı fault zones* (*SdFZ*): The WNW–ESE to E–W-striking KFZ and SdFZ are developed in the southern part of the Yaka area (Fig. 10a). They can be traced 3–5 km inside the

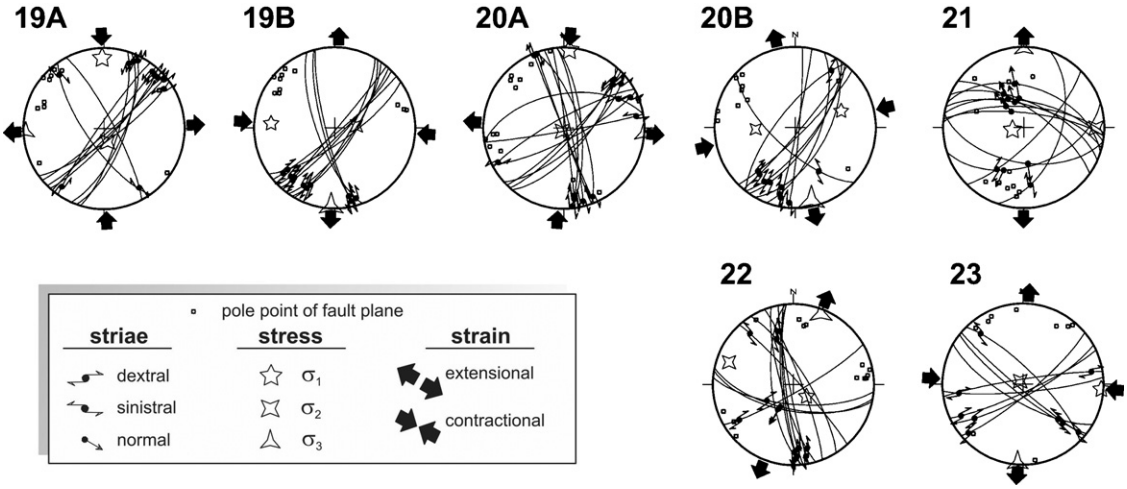

Fig. 11. Lower-hemisphere equal-area projection of fault planes, slickenlines, and constructed palaeostress configurations for the Yaka area.

mapped Yaka area, but the actual lengths are more than a few tens of kilometers. In fact, according to Sözbilir et al. (2011) they are the westernmost rims of the extensional normal faults that bound the modern Gediz graben (Figs. 1 and 2). In this study, we provide new 11 fault plane data for the KFZ and SdFZ (projection 21 in Fig. 11). In the Yaka area, the SdFZ is characterized by a 4 km long, 1 km wide high-angle fault, and includes three sub-parallel faults. The observed fault planes dip at an average angle of 65°SW.

In the study area, the KFZ is a 500 m wide, 1.5 km long, graben-bounding normal fault cross-cutting the NE–SW striking fault (Fig. 10a). The fault displays locally well-preserved slickensided surfaces revealing that the KFZ is a normal fault dipping at an average angle of 70°NE. Along the SdFZ and KFZ, the upper sequence of the Miocene units is displaced and is juxtaposed tectonically with Quaternary sediments exposed on down-thrown blocks.

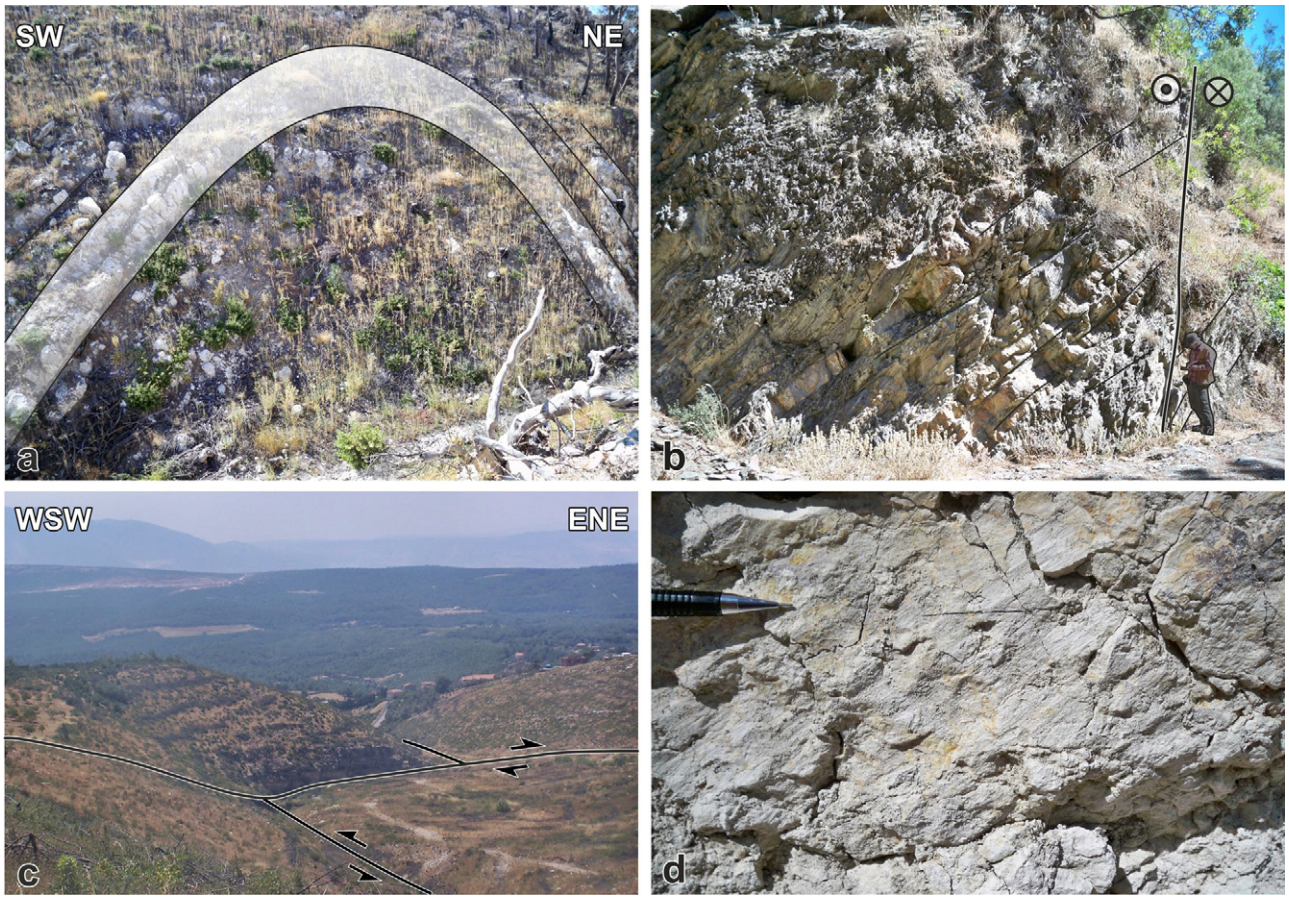

Fig. 12. Field photos of post-Miocene structures from the Yaka area. (a) Close up view of an approximately E–W trending fold in the Yaka formation. (b) Nearly vertical fault plane of the NE striking Karaçay fault zone cutting the Bornova Flysch Zone. (c) A field photo showing the left-lateral offset of a N–S striking fault along the NE striking cross fault. (d) Close up view of a NW striking strike-slip fault plane including well-developed slickenlines.

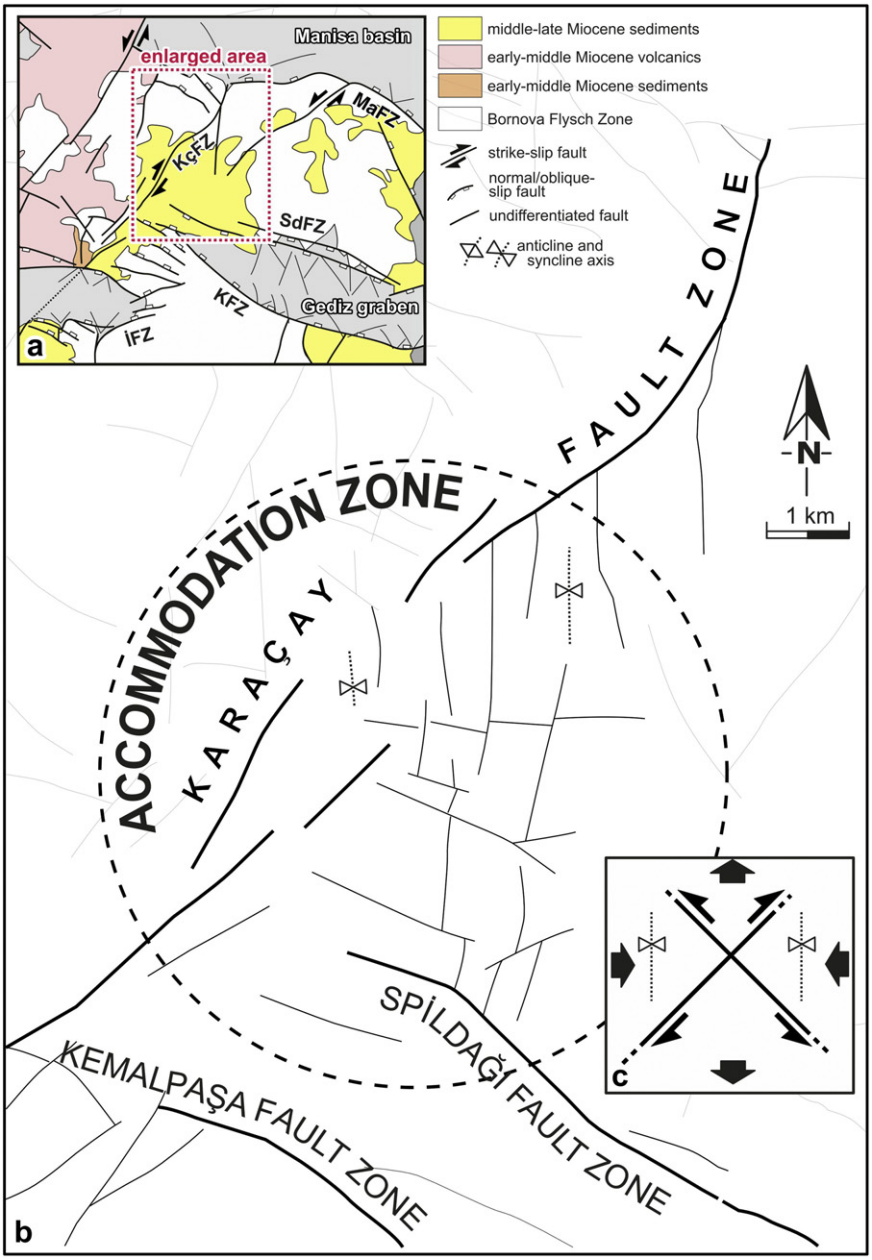

Fig. 13. Interpretation of fault interactions in the Yaka area (a, inset). (b) Interaction of the Spildağı fault zone with the Karaçay fault zone by a number of N–S striking left-lateral strike-slip faults, (c) simplified model to illustrate the development of N–S folds caused by E–W compression (convergent arrows) and N–S extension (divergent arrows) within the Yaka area.

Cross-faults: These structures are mapped in a triangular area between the Manisa fault zone in the N, the KçFZ in the NW and the SF in the S as three different fault subsets that have NE–SW, NW–SE and N–S strikes (Fig. 10a). Generally, the lengths of these faults can be traced to a maximum of 3 km. The cross-faults displace the Miocene volcano-sedimentary units and laterally offset the fold axes of Miocene strata. According to the collected 27 fault plane data along these structures (see projections 22 and 23 in Fig. 11), NE-striking ones have a left-lateral component, while the NW-trending faults also have a normal fault character but with a right-lateral component (Fig. 12c and d). The third, N–S striking subset has a left-lateral strike-slip character. These second-order faults developed as accommodation structures inside the triangle area formed by the junction of SdFZ, KFZ and KçFZ; it forms the connection of the major normal and strike-slip faults (Fig. 13).

Folds: Two distinct fold patterns are developed in the Yaka area. These are N–S trending folds that are developed in the lower sequence of Miocene strata, and approximately E–W trending folds observed only in the lacustrine limestones of the Yaka Formation which is the highest unit of the upper sequence (Fig. 10a). The N–S trending folding is observed within the Sabuncubeli and Kızıldere Formations around the NE of Beşyol village. They are mostly open synclines gently plunging to the N and they are parallel to the nearby faults. The fold axes can be traced over at least 1 km and are overlain by the clastics of the Kızılca Formation. The E–W-trending folds are well exposed between the Yaka and Beşyol villages where they are nearly parallel to NW–SE-trending normal faults (Fig. 10a). They are relatively large, open and plunging gently both towards the northwest and to southeast (Fig. 12a). Towards the north the folds become more open with interlimb angles around 130°. The development of the E–W trending folds are interpreted to be forced

folds that developed on the rotating faults blocks, similar to the mechanism proposed for folds in the Menemen area (Fig. 7c). A similar extensional folding mechanism is also proposed for the folds in the Gediz graben (Seyitoğlu et al., 2000; Sözbilir, 2001, 2002; Çiftçi and Bozkurt, 2008). On the other hand, the N–S folds that trend parallel to the secondary faults within the accommodation area of the KçFZ and SdFZ make an angle of approximately 45° with both major fault zones (Fig. 13).

5. Palaeostress configurations

In the key areas we studied, we have collected more than 320 fault slip data (Table 1). We have joined our data with published palaeostress data sets (Table 2). Among these, our sites which are labeled as 1–12 belong to the Karaburun area and they have produced 17 palaeostress configurations. Sites 13–18 belong to the Menemen area have generated 6 palaeostress configurations. Sites 19–23 are located within the Yaka area and they yielded 7 palaeostress configurations (Fig. 14a).

The results of the palaeostress analyses are depicted in Figs. 6, 9 and 11 and Table 1. As described in previous sections, during the field studies we encountered overprinting slickensides in seven locations and they are analyzed separately. These overprinting relationships, together with cross-cutting relationships and stratigraphic information, are used to determine the various deformation phases and their succession in time. However, deformation phases of areas where no cross-cutting or overprinting relationships were encountered were based on the age of host lithology, and the similarity of the stress orientations and stress ratios to other sites for which the deformation phase was already assigned precisely (cf. Sperner and Zweigel, 2010).

Within the studied sub-areas around the İBTZ, during the late Cenozoic (Miocene–Quaternary) interval, three different deformation phases have been recognized based on our kinematic analyses and available palaeostress data from literature (Bozkurt and Sözbilir, 2006; Özkaymak and Sözbilir, 2008; Sözbilir et al., 2008, 2011; Uzel and Sözbilir, 2008; Uzel et al., 2012).

The first phase (Phase 1) is characterized by N–S directed extension and E–W contraction and likely took place during the early (?) to late Miocene. This transtensional phase formed several volcano-sedimentary basins. It was followed by a second phase (Phase 2) which caused wrench- to extension-dominated transtension. The structures related to Phase 2 are observed all around İzmir Bay and probably took place during the early Pliocene. The last deformation phase (Phase 3) is characterized by both NW–SE left-lateral and NE–SW right-lateral strike-slip faults and E–W trending normal faults, causing a transtensional deformation phase.

5.1. Phase 1

Phase 1 is well documented in two areas, in the Kocaçay basin and along the Orhanlı fault zone (OFZ) which forms the western margin of the Cumaovası basin. In the Kocaçay basin, two sites along the Mahmutdağı fault zone (58 and 59; Fig. 14a) from Sözbilir et al. (2011) at the eastern margin of the İBTZ, provide evidence for two families of faults: NE-trending dextral strike-slip faults and low-angle normal faults. The INVD technique identifies steeply plunging σ_2 axes (71°), but gently plunging σ_1 and σ_3 axes (18° and 08°). The results suggest that strike-slip faulting developed under an approximately N–S-trending extension associated with E–W contraction (Table 2b). The fault-slip measurements for the low-angle normal faulting define a near horizontal σ_3, trending approximately 223° with a 15° plunge, whereas σ_1 and σ_2 axes have attitudes of approximately 080°/72° and 316°/11°, respectively. The results suggest a NE–SW directed extension. Phase 1 faults are kinematically congruent with the N–S extensional direction expected to have been associated with the opening of the supra-detachment basins during the early Miocene, an interpretation that is supported by the σ_3 orientation calculated for strike-slip faults.

Structures related to Phase 1 were also documented along the Orhanlı fault zone (OFZ) which forms the western margin of the Cumaovası basin and is the most prominent structure in the region south of İzmir city. Along the Orhanlı fault zone, crosscutting relationships and superposition of successive striae in fault planes show that sinistral faulting was reactivated as right-lateral strike-slip faulting (Uzel and Sözbilir, 2008). The older kinematic structures including sinistral shear sense were determined in Sites 38, 39, 40, 41 and 44 (Fig. 14b and Table 2a). The inverse analysis results of fault-slip measurements for the early phase of sinistral strike-slip faulting define steeply plunging σ_2 axes (53° and 76°), but gently plunging σ_3 axes (09° and 32°). The main orientation of the σ_1 axis is very variable with an approximately horizontal plunge (10° and 30°). The results suggest that sinistral strike-slip faulting developed under an approximately N–S trending contraction regime associated with E–W extension. The fault-slip measurements for the later phase of dextral strike-slip faulting define a near horizontal σ_1, trending approximately 260° with a 10° plunge, whereas σ_3 axes have attitudes of approximately 160°/10°, respectively. The orientation of σ_2 axes is variable with approximately vertical plunging. The results suggest an approximately N–S directed extension associated with E–W contraction (Table 2a).

5.2. Phase 2

Deformation Phase 2 is characterized by an association of strike-slip and oblique- to dip–slip normal faults that deformed the Miocene units. Eight sites (1A, 4A, 5A, 7A, 9–12, 15–18, 19A, and 20A; Fig. 14a and Table 1) along the KbFZ, KrFZ, HFZ and their subsets characterize this phase in the Karaburun and Menemen subareas (Fig. 14b). These NE and NW striking fault zones seem to form conjugate sets since they operated at the same time and had right- and left-lateral strike-slip character, respectively. The palaeostress configurations computed from the data of the Karaburun and Menemen areas are reasonably coherent, and define a horizontal component of the σ_3 axes ranging between N20°W and N15°E, with a plunge of <22°. The plunge of the σ_1 axes is nearly vertical (>56°) in most sites of the Karaburun area, whereas in the Menemen area the plunge of σ_1 is sub-horizontal (<17°).

The computed data from Yaka area along the KçFZ, however, indicate that here the intermediate (σ_2) stress is steeply plunging. The overall results suggest that in all areas the direction of minimum stress (σ_3) is horizontal and approximately NE–SW to E–W, while in the Karaburun and Menemen areas σ_1 is more or less subvertical. In the Yaka area, the direction of σ_3 is horizontal, in a NNW–SSE direction (Table 1). The second phase is attributed to the early Pliocene, based on kinematic/stratigraphical information and the geological context of the region by Bozkurt and Sözbilir (2006).According to their palaeostress analyses, and the subsequent analyses of Uzel and Sözbilir (2008), Özkaymak and Sözbilir (2008) and Sözbilir et al. (2011) at several sites of the eastern part of the İzmir Bay (sites 24–27, 38–42, 56, and 60–64 in Fig. 14a), the E–W extension and related N–S contractional strain across the region is also related to early Pliocene events as revealed by reactivated structures (Fig. 14b).

5.3. Phase 3

In this deformation phase, palaeostress orientations which indicate both extensional and strike-slip deformation are obtained (Fig. 14b, and Table 1), similar to what happened during Phase 2,

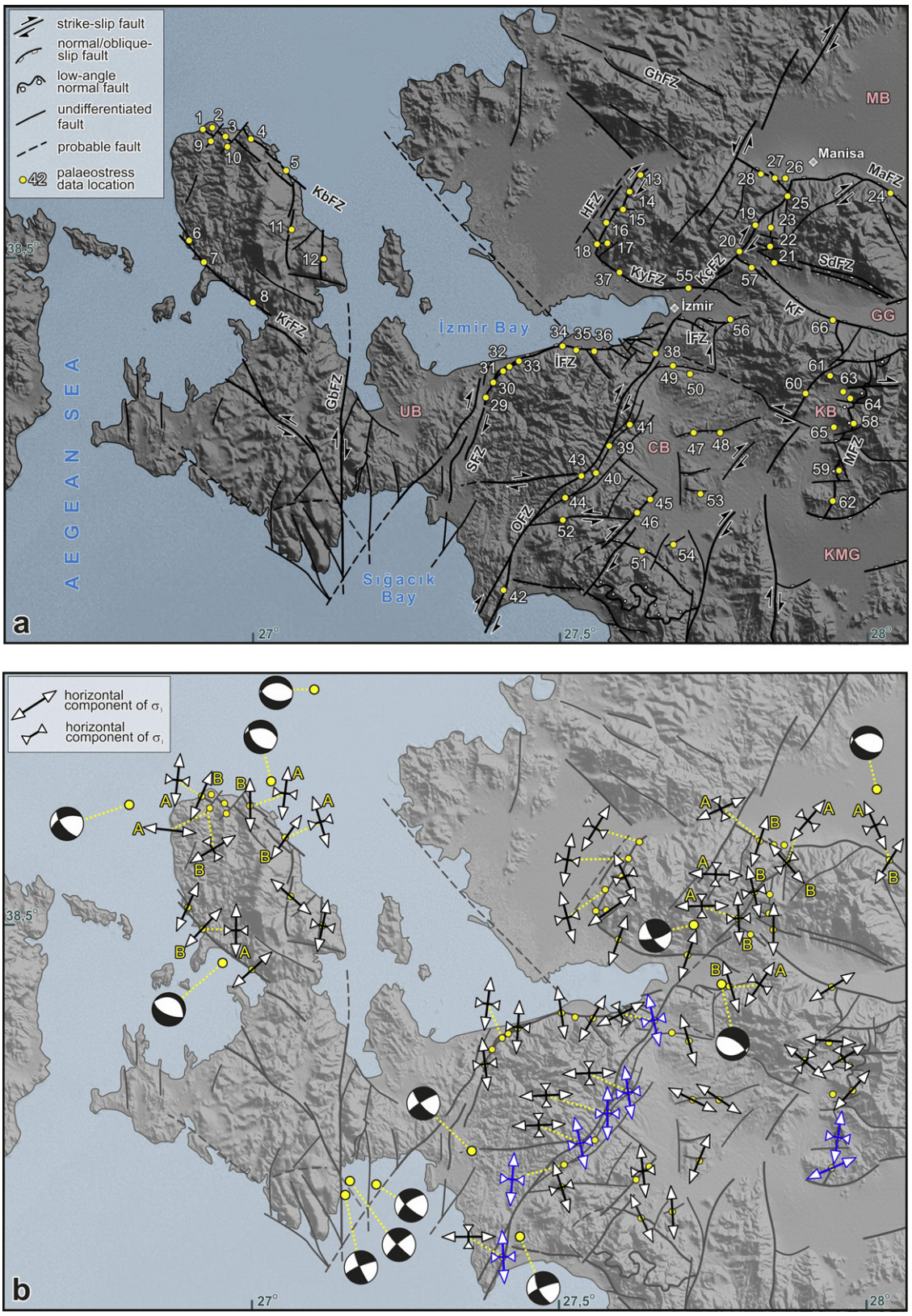

Fig. 14. Orientation and temporal variation of horizontal components of principal palaeostrain axes. (a) Distribution of palaeostress data sites draped on a simplified tectonic map of İzmir Bay area. KbFZ, Karaburun fault zone; KrFZ, Karareis fault zone; HFZ, Harmandalı fault zone; GbFZ, Gülbahçe fault zone; GhFZ, Güzelhisar fault zone; KyFZ, Karşıyaka fault zone; SFZ, Seferihisar fault zone; OFZ, Orhanlı fault zone; İFZ, İzmir fault zone; KF, Kemalpaşa Fault; SdFZ, Spildağı fault zone; MaFZ, Manisa fault zone; MFZ, Mahmutdağı fault zone; UB, Urla Basin; CB, Cumaovası Basin; KMG, Küçük Menderes Graben; KB, Kocaçay Basin; GG, Gediz Graben; MB, Manisa Basin. (b) Calculated horizontal component of maximum and minimum strain axes directions. Blue arrows related to Miocene faulting along the Mahmutdağı and Orhanlı fault zones (Phase 1). A (B) refers to the older (younger) faulting on reactivated fault planes. The focal mechanism solutions (beachballs) of the main earthquakes are used to identify recent tectonic activity (Tan et al., 2008). Characteristics of local stress states are shown in Tables 1 and 2. (For interpretation of the references to color in this figure legend, the reader is referred to the web version of the article.)

Table 1
Characteristics of stress states used to reconstruct the stress regimes as illustrated in Figs. 6, 9 and 11. #, Number of fault slip data; D° and P°, dip and plunge of stress axes in degrees; Φ, ratio of stress magnitude differences [$\Phi = (\sigma_2 - \sigma_3)/(\sigma_1 - \sigma_3)$]. RUP and ANG are quality estimators: average ANG values below 25° and average RUP values below 50% indicate good fits between computed shear stress and actual fault slip data. Rej, number of rejected data because of the low quality.

Site	Name of fault	Principle stress axes (dip°/plunge°)			Φ	#	Max ANG	Max RUP	Rej
		σ_1	σ_2	σ_3					
Karaburun area									
1A	Karaburun fault zone	289/56	091/33	187/09	0.527	14	16	48	2
1B	Karaburun fault zone	235/74	118/08	026/14	0.328	12	24	43	1
2	Karaburun fault zone	087/20	221/62	350/18	0.882	07	14	30	0
3	Karaburun fault zone	276/55	109/34	015/06	0.659	16	10	38	1
4A	Karaburun fault zone	105/13	234/69	011/15	0.691	10	18	41	1
4B	Karaburun fault zone	179/72	327/15	059/09	0.346	12	22	48	0
5A	Karaburun fault zone	081/26	229/60	344/14	0.874	07	23	43	0
5B	Karaburun fault zone	265/72	138/11	046/14	0.476	06	19	38	1
6	Karareis fault zone	306/52	107/36	204/09	0.723	07	12	44	0
7A	Karareis fault zone	266/61	072/29	165/06	0.944	11	11	22	1
7B	Karareis fault zone	010/69	154/17	247/12	0.322	07	17	23	1
8	Karareis fault zone	354/76	144/12	235/07	0.640	07	11	23	0
9A	Karareis fault zone	015/83	191/07	281/01	0.575	12	21	47	1
9B	Karareis fault zone	088/87	316/02	226/02	0.749	8	19	36	1
10	West Karaburun	142/69	006/16	271/13	0.520	6	21	39	0
11	West Kösedere	297/75	029/11	119/15	0.523	10	16	44	4
12	West Mordoğan	032/67	286/07	193/22	0.454	11	16	42	3
Menemen area									
13	Harmandalı fault zone	306/06	090783	215/04	0.821	10	16	40	3
14	Harmandalı fault zone	254/11	029/75	162/11	0.620	22	24	47	7
15	East Koyundere	108/81	328/07	237/06	0.833	12	23	45	4
16	Harmandalıfault zone	064/17	287/68	158/14	0.835	10	14	43	5
17	Southeast Ulucak	142/80	326/10	236/01	0.749	06	22	48	0
18	Harmandalı fault zone	099/10	255/79	009/04	0.807	22	22	40	3
Yaka area									
19A	Karaçay fault zone	353/11	161/79	263/02	0.547	11	15	41	1
19B	Karaçay fault zone	285/25	085/63	191/08	0.764	11	18	48	2
20A	Karaçay fault zone	017/03	250/84	107/05	0.459	15	19	44	8
20B	Karaçay fault zone	064/31	266/57	160/10	0.841	10	21	39	1
21	Kemalpaşa & Spildağı Faults	241/70	091/17	358/10	0.458	11	12	28	3
22	East Beşyol	102/88	295/02	205/01	0.840	13	23	40	4
23	North Beşyol	286/02	036/86	196/04	0.842	09	17	39	3

but the other way around. This phase, which is evidenced by the youngest structures of the region, indicates transtensional deformation within the İBTZ. The orientation of extensional strain axes varies between NNW–SSE to NNE–SSW, while contractional strain directions in sites with a strike-slip solution vary from WNW–ESE to ENE–WSW. Having both extensional and coeval strike-slip deformation implies that Phase 3 is transtensional in nature. This phase postdates Phase 2, and seems to have been active during the late Pliocene–Quaternary time interval (Sperner et al., 2003; Aktuğ and Kılıçoğlu, 2006; Tan et al., 2008; Heidbach et al., 2010). The palaeostress configurations from KbFZ, KrFZ, KçFZ, KFZ, SdFZ and some secondary faults sampled in sites 1B, 2, 3, 4B, 5B, 6, 7B, 8, 9B, 13, 14, 19B, 20B, 21–23 (Figs. 6, 9, 11 and 14a) indicate a combination of an extensional and strike-slip deformation (Fig. 14b, and Table 1). These fault zones belong to the youngest deformation phase and are the faults fringing İzmir Bay. We therefore conclude that İzmir Bay has developed during the last deformation phase in response to transtensional deformation in the region, as suggested previously (Bozkurt and Sözbilir, 2006; Uzel and Sözbilir, 2008; Özkaymak and Sözbilir, 2008; Sözbilir et al., 2011) based on major Quaternary basin bounding faults in the region (Fig. 14a and b, and Table 1).

5.4. Spatio-temporal relationships

In the late Cenozoic, two different deformation styles and three different deformation phases have been recognized in the studied areas around İzmir Bay. During Phase 1, all studied subareas were dominated by strike-slip faulting and related structures. For Phases 2 and 3, however, there is structural consistency between the Menemen and Yaka subareas within the İBTZ, in the sense that these areas were dominated by strike-slip tectonics, whereas the Karaburun area outside of the İBTZ was dominated by extensional deformation during Phase 3. The geometry and kinematics of brittle structures in the Karaburun Peninsula are consistent with wrench-dominated deformation. Simple shear within the zone is accommodated by right-lateral *R* shear (NE–SW trending faults) and left-lateral *R′* shear (NW–SE trending faults). Riedel shear developing at a small angle to the main fault zone is synthetic to the main fault with the same shear sense. Conjugate Riedel shear (NW–SE trending) faults are antithetic fractures that are oriented to the main fault at high angles and have a shear sense opposite to that of the main fault. The documented reactivation on some of the NW–SE trending faults in the Karaburun Peninsula predicts that *R′* shear initiated as left-slip shear fractures and later evolved to normal oblique-slip faults, possibly caused by vertical axis rotation. This can be explained by the progressive deformation produced by the switch from wrench- to extension- dominated transtension. This new local strain field favours the development of new dip- to oblique-slip normal faults or reactivation of the earlier strike-slip faults. This relationship implies that the Karaburun area was kinematically detached from the eastern areas at the end of deformation Phase 2, by the Pliocene. After the initiation of Phase 2, differential stretching between the Menderes Massif and the area west of it, including İzmir Bay, caused the İBTZ to develop as a transfer zone (Fig. 15). Most probably, dominance of strike-slip deformation during Phases 1 and 2, within and outside the İBTZ, implies that the İBTZ evolved from a wider shear zone into a relatively narrow discrete fault zone by the late Pliocene, during which the strike-slip and extensional

Table 2
Published palaeostress tensors used for the reconstruction of the deformational history of İzmir Bay area. #, Number of fault slip data; D° and P°, dip and plunge of stress axes in degrees; Φ, ratio of stress magnitude difference [$\Phi = (\sigma_2 - \sigma_3)/(\sigma_1 - \sigma_3)$]. Reference codes are: (1) Bozkurt and Sözbilir (2006), (2) Özkaymak and Sözbilir (2008), (3) Sözbilir et al. (2008), (4) Uzel and Sözbilir (2008), (5) Uzel et al. (2012), and (6) Sözbilir et al. (2011).

Site	Name of fault	Principle stress axes (dip°/plunge°)			Φ	#	Reference
		σ_1	σ_2	σ_3			
Manisa Basin (Gediz Graben)							
24A	Manisa fault zone	259/35	058/53	162/10	0.622	9	1
24B	Manisa fault zone	208/83	303/01	033/07	0.245	14	1
25A	Karaçay fault zone	136/02	261/86	046/03	0.922	11	2
25B	Karaçay fault zone	228/08	357/78	136/09	0.798	10	2
26	Manisa fault zone	199/72	303/05	036/17	0.195	8	2
27A	Manisa fault zone	173/19	024/68	267/10	0.721	8	2
27B	Manisa fault zone	343/75	091/04	182/14	0.110	8	2
28A	Manisa fault zone	130/65	336/22	242/10	0.630	10	2
28B	Manisa fault zone	256/70	113/16	020/12	0.353	11	2
İzmir Bay							
29	Seferihisar fault zone	262/08	084/82	352/00	0.644	6	3
30	Seferihisar fault zone	139/68	252/09	345/20	0.268	6	3
31	Seferihisar fault zone	088/13	341/52	187/65	0.509	10	3
32	Seferihisar fault zone	201/67	100/04	008/23	0.265	6	3
33	Seferihisar fault zone	089/07	344/65	182/24	0.432	6	3
34	İzmir fault zone	178/62	350/28	082/04	0.150	6	3
35	İzmir fault zone	111/73	276/17	008/04	0.104	6	3
36	İzmir fault zone	131/67	300/22	031/04	0.271	6	3
37	Karşıyaka fault zone	326/73	108/13	200/10	0.280	7	3
Cumaovası Basin							
38A	Orhanlı fault zone	163/17	276/53	062/32	0.613	6	4
38B	Orhanlı fault zone	257/06	014/77	166/11	0.315	6	4
39A	Orhanlı fault zone	360/23	162/66	267/06	0.716	6	4
39B	Orhanlı fault zone	260/40	098/48	001/09	0.651	6	4
40A	Orhanlı fault zone	185/05	291/72	094/17	0.565	6	4
40B	Orhanlı fault zone	278/39	095/51	187/01	0.626	6	4
41A	Orhanlı fault zone	355/15	206/72	088/09	0.336	6	4
41B	Orhanlı fault zone	267/22	063/66	173/09	0.579	6	4
42A	Orhanlı fault zone	358/04	261/64	090/26	0.434	6	4
42B	Orhanlı fault zone	265/17	096/73	356/03	0.212	6	4
43A	Orhanlı fault zone	355/15	206/72	088/09	0.336	6	4
43B	Orhanlı fault zone	258/11	066/78	167/02	0.821	6	4
44	Orhanlı fault zone	275/14	086/76	185/02	0.688	6	4
45	Orhanlı fault zone	259/03	154/77	350/12	0.516	6	4
46	Orhanlı fault zone	106/07	350/74	198/15	0.715	6	4
47	Kısıkköy fault	020/69	218/20	126/06	0.320	6	4
48	Kısıkköy fault	023/65	205/25	114/00	0.182	6	4
49	Buca fault	208/53	079/25	336/25	0.080	6	4
50	Buca fault	154/62	250/03	341/27	0.520	6	4
51	Değirmendere fault	225/73	065/16	333/06	0.220	6	4
52	Deliömer fault	074/18	239/72	342/04	0.252	6	4
53	Conjugate set	094/66	298/22	204/09	0.336	6	4
54	Conjugate set	010/68	267/15	175/21	0.316	6	4
İzmir Bay							
55	Karşıyaka fault zone	315/78	110/10	200/05	0.431	9	5
56A	İzmir fault zone	129/18	301/71	038/02	0.278	7	5
56B	İzmir fault zone	182/73	073/06	341/16	0.328	9	5
Kocaçay Basin							
57	Kemalpaşa fault	334/82	096/04	187/07	0.499	6	5
58	Mahmutdağı fault zone	080/72	316/11	223/18	0.418	5	6
59	Mahmutdağı fault zone	096/18	300/71	188/08	0.388	6	6
60	Kesmedağı fault	222/04	116/76	313/13	0.279	5	6
61	Kalkancatepe fault	291/74	186/04	095/16	0.469	8	6
62	Karabeldere fault	057/72	156/03	247/18	0.168	7	6
63	Dereköy fault	152/06	036/77	243/12	0.139	12	6
64	Dereköy fault	027/78	134/04	225/12	0.363	11	6
65	Karaot fault	094/22	336/50	199/32	0.652	7	6
66	Spildağı fault zone	222/82	332/03	06208	0.702	11	6

deformation completely decoupled from each other. In addition, the faults that control the margins of the inner and outer parts of the İzmir Bay have been active during the latest deformation phase since the late Pliocene. These faults generally have a normal component but are connected to NE–SW right-lateral strike-slip faults. This implies that İzmir Bay is a transtensional basin developed in response to synchronous strike-slip/normal faulting along the İBTZ.

6. Discussion and conclusions

The İBTZ is a NE–SW trending pre-existing strike-slip dominated zone of weakness that marks the lateral termination of E striking graben-faults and linked spatially discrete loci of extension. The first field-based studies of Kaya (1979, 1981) reported that the region between İzmir and Balıkesir was divided into NNE-trending depressions of Neogene age by steep, oblique-slip faults

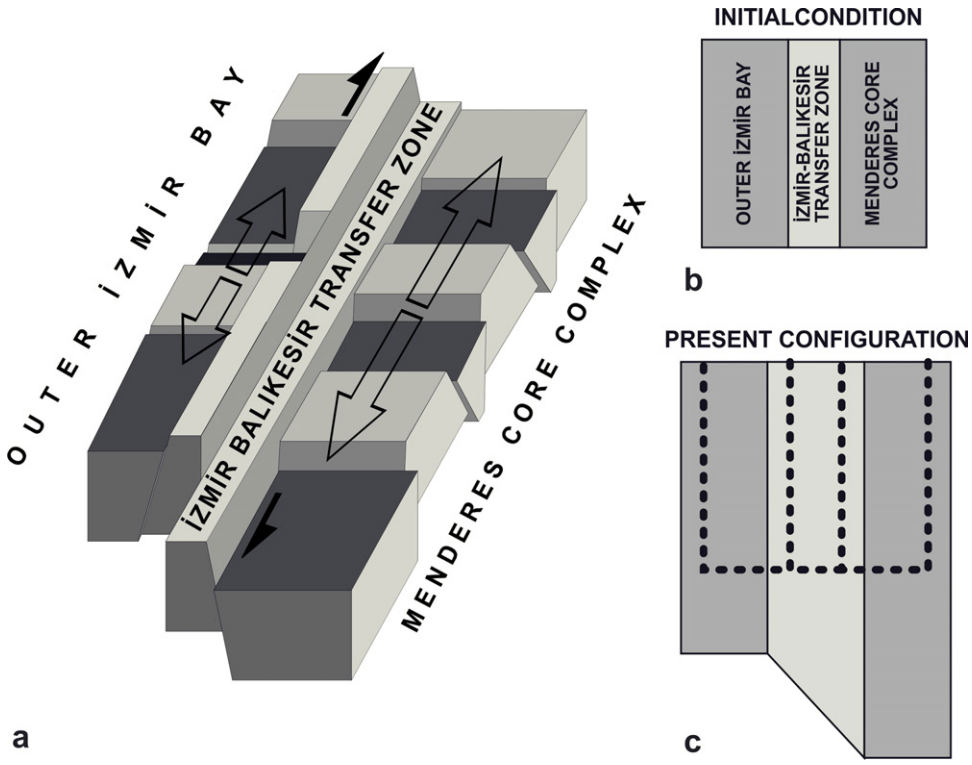

Fig. 15. (a) Differential stretching model proposed for the development of İzmir–Balıkesir Transfer Zone and decoupling between the Menderes Core Complex and Outer İzmir Bay (mainly Karaburun) area. Plan views of the model are shown from (b) initial conditions, and (c) present configuration. Note that the extension in the Menderes Core Complex is considerably larger than the extension in the Outer İzmir Bay area, and therefore the strain in the İBTZ is not homogenous.

with a considerable left-lateral strike-slip component. He indicated that these faults seemed older than the E–W to WNW normal faults and hence might follow older structural trends. These major strike-slip cross-faults offset the main Gediz detachment fault near its western end, and Şengör (1987) delineated them as a transfer fault zone. This zone might be classified as a transverse or replacement structure, defined by Şengör et al. (1985) as a configuration coincident in space with palaeotectonic structures but that does not have the same function during a later tectonic episode. Its origin may be attributed to the influence of the basement structure inherited from the transform nature of the zone during the late Cretaceous. This is supported by faults within the İBTZ which may have their earliest record in the Late Cretaceous convergence, related to an existing transform zone perpendicular to the Neotethys. It later acted as a wrench- to extensional-dominated transfer fault zone during the late Cenozoic (Okay et al., 1996; Ring et al., 1999; Uzel & Sözbilir, 2008; Özkaymak & Sözbilir, 2008; Uzel et al., 2012; Özkaymak et al., in press; Okay et al., in press).

The İBTZ is composed of NE–SW elongated Miocene volcano-sedimentary basins that are dissected by mainly E–W elongated Plio–Quaternary depressions. Miocene stratigraphy is typified by a folded (normal and strike-slip faulted) volcano-sedimentary sequence characterized by coal-bearing clastic to carbonate sediments, andesitic to rhylotic pyroclastic deposits and lava flows, and lacustrine carbonates. The younger and recent basin-fill is represented by continental alluvial to fluvial deposits and coastal clastics of the Aegean sea.

The Neogene–Quaternary evolution of the zone is characterized by variable wrench to extension dominated transtension, and has resulted in a complex fault pattern. Three different deformation phases have been encountered around İzmir Bay area for the late Cenozoic time interval.

In addition, we have combined our new data from the İBTZ with published data from western Anatolian grabens and the southwest Aegean to produce a Late Cenozoic kinematic map of the region (Fig. 16). A major crustal-scale NE–SW-trending right-lateral strike-slip shear zone, the Mid-Cycladic Lineament (MCL), southeast of the İBTZ has been interpreted by Pe-Piper et al. (2002) to mark the boundary between the eastern and western Aegean (Fig. 16; Morris and Anderson, 1996). The MCL ceased activity in the latest Miocene–Early Pliocene coevally with the development of the North Anatolian fault (Walcott and White, 1998). Regional kinematic studies have also suggested that a major change in the kinematics of the Aegean occurred in the latest Miocene–early Pliocene (Le Pichon et al., 1995).

The oldest stage of deformation (Phase 1) is characterized by strike-slip deformation which is controlled by vertical intermediate stress, E–W contraction and N–S extensional strain axes. Faults of this phase controlled the location of the NE–SW trending episodic nature of eruption centres. During this stage, the eastern margin of the İBTZ underwent transtensional deformation that was characterised by kinematically linked E–W trending low-angle normal faults and NE–SW trending strike-slip faults in the Kocaçay basin (Sözbilir et al., 2011). Major movement along the nearby Gediz detachment also occurred at this time. This was associated with the denudation of metamorphic core complexes in the footwalls of the Gediz and Büyük-Menderes Detachment Faults (Hetzel et al., 1995; Emre and Sözbilir, 1997; Koçyiğit et al., 1999; Lips et al., 2001; Sözbilir, 2001, 2002; Seyitoğlu et al., 2002; Işık et al., 2003, 2004; Bozkurt and Sözbilir, 2004). The footwall metamorphic rocks were progressively mylonitised, exhumed, and intruded by syn-deformational granitoids, the Turgutlu and Salihli granodiorites. The Salihli granodiorite yielded a wide range of ages, all obtained from the same granitoids: ^{39}Ar–^{40}Ar amphibole isochron and biotite plateau cooling ages of 19.5 ± 1.4 and 12.2 ± 0.4 Ma (Hetzel et al., 1995), U-Pb crystallization ages of 15.0 ± 0.3 Ma from allanite (Glodny and Hetzel, 2007), and Th–Pb ion microprobe monazite ages ranging from 21.7 ± 4.5 Ma to 9.6 ± 1.6 Ma (Catlos

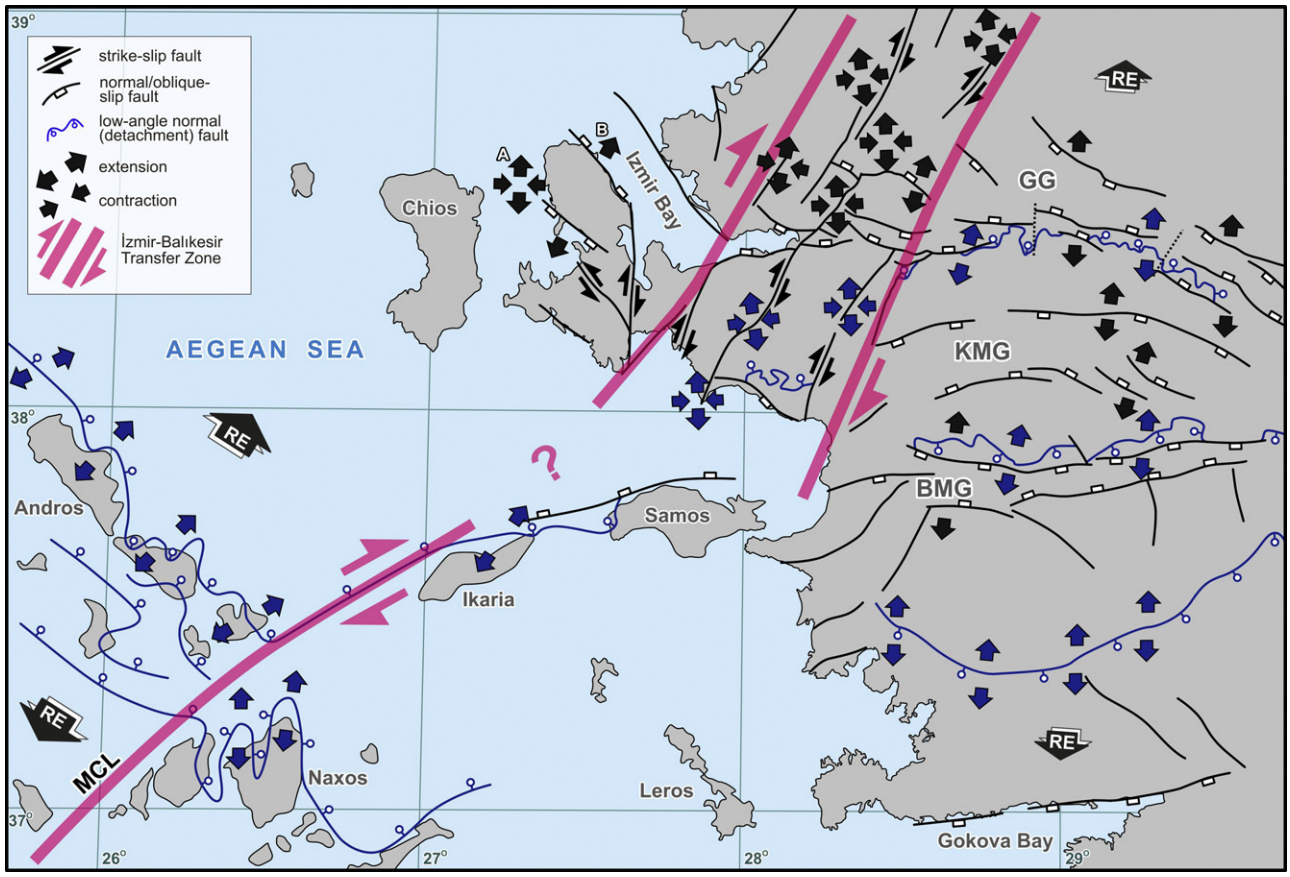

Fig. 16. Miocene (blue arrow) and post-Miocene (black arrow) kinematic data from the İBTZ combined with published data from the Aegean and West Anatolian Extensional Systems (Walcott and White, 1998; Bozkurt and Satır, 2000; Lips et al., 2001; Sözbilir, 2002; Ring et al., 2003; Bozkurt and Sözbilir, 2004, 2006; Emre and Sözbilir, 2007; Uzel and Sözbilir, 2008; Gürer et al., 2009; Jolivet et al., 2010; Sözbilir et al., 2011; Uzel et al., 2012). Miocene extensional detachment faults show NE–SW oriented regional extension (RE) that parallel the Mid-Cycladic Lineament (MCL) while a NNE–SSW oriented regional extension (RE) has been documented in the West Anatolian Extensional System, east of the İBTZ. A (B) refers to the older (younger) faulting around Karaburun Peninsula. (For interpretation of the references to color in this figure legend, the reader is referred to the web version of the article.)

et al., 2010). This timing of the syn-extensional magmatism in the footwall of the Gediz detachment coincides with a period of widespread volcanism between 21.5 and 9 Ma in the NE trending transtensional basins located within the İBTZ. The available radiometric age data placed Phase 1 into 21.5–9 Ma, and suggest that when the E–W trending grabens developed under the control of the NNE–SSW pure extension, the İBTZ underwent N–S strike-slip dominated transtension (Fig. 16). Both the end of the activity of the Mid-Cycladic Lineament and a concurrent major change in the kinematics of the Aegean occurred in the latest Miocene–early Pliocene. In contrast to the MCL, however, the activity of the İBTZ has continued until today.

The second stage of deformation (Phase 2) closely follows the major change in Aegean kinematics in time and is characterized by two different stress configurations: a strike-slip regime inside the İBTZ and an extensional regime outside of it. It prevailed during the early Pliocene because the strike-slip faults cut and displaced the late Miocene lacustrine carbonates. Even though the regional stress field has been essentially characterized by a sub-vertical maximum principal stress axis, the İBTZ induced differences in the stress field during Phase 2. Within the fault zone, palaeostress analysis points to a local stress field with NW–SE subhorizontal compression and NE–SW sub-horizontal tension. With increasing finite strain intensity, the former wrench-dominated transtension changed to extension-dominated transtension where maximum extension direction is always horizontal, but the maximum shortening direction changed with time. Available palaeostress analyses of the post-Miocene faults along the E–W trending grabens suggest that they were formed under the control of N–S to NNE–SSW extension, which is compatible with the regional N–S extension. However, in the western end of the grabens, within the İBTZ, wrench- to extension-dominated transtension was prevailing (Fig. 16). This was associated with a shift from wrench- to extension-dominated deformation within the İBTZ. Field evidence also suggests that some older strike-slip faults may be reactivated as oblique-slip normal faults caused by a switch from strike-slip to extension-dominated deformation. The timing of Phase 2 can be correlated both with the ending of MCL activity and with the onset of N–S rifting in the West Anatolian Extensional System that occurred between 5 and 7 Ma (Lips et al., 2001; Armijo et al., 1999). The $^{40}Ar/^{39}Ar$ ages of syn-extensional muscovites in the footwall rocks of the Gediz detachment fault, of 6.7 ± 1.1 Ma and 6.6 ± 2.4 Ma constrain the timing of late-stage extension and the reactivation of the Gediz detachment fault (Lips et al., 2001). In addition, Gessner et al. (2001) presented two zircon and apatite fission-track ages of 5.2 ± 0.3 Ma from the Salihli granitoid that show accelerated cooling rates in the central Menderes Massif in the earliest Pliocene. These results strongly indicate that the last exhumation of the central Menderes Massif under the footwall of the Gediz Detachment Fault was coeval with the Plio–Quaternary transtension within the İBTZ.

The youngest stage of deformation (Phase 3) occurs from the late Pliocene onwards. The eaarlier strike-slip dominated regime (Phase 2) is then replaced by this younger extension-dominated transtensional deformation phase, producing grabens in the early

Pleistocene (Özkaymak et al., in press). Inside the IBTZ, the extension caused segmentation into two branches: the western end of the Gediz Graben (e.g. Kocaçay and Manisa basins) and the Inner İzmir Bay. Outside the IBTZ, Phase 3 is characterized by dominantly extensional deformation, resulting in the development and growth of the Outer İzmir Bay and the Gediz Graben.

The İBTZ was almost always dominated by right-lateral strike-slip faulting during the late Cenozoic except for Phase 2 during which it locally acted as a left-lateral strike-slip transfer zone. On the basis of existing and our new stratigraphical and kinematical data, we conclude that İzmir Bay originated in the Pliocene as a transtensional basin., In response to local transtension along the İBTZ, extensional terranes on either side of the zone started, caused by differential stretching. The moment tensor solutions for recent earthquakes corroberate that strike-slip motions along NE–SW and NW–SW trending strike-slip faults coexist with dip-slip E–W trending faults. This regime agrees well with the regional extensional framework related to NNE–SSW crustal stretching.

Recently started paleomagnetic and geochronological studies are aimed at: (1) establishing the amount and timing of block rotations inside and outside the İBTZ and (2) discovering if there is any structural and kinematic relationship between the MCL and İBTZ.

Acknowledgements

This work is a part of the PhD study of Bora Uzel and it is supported by the Scientific and Technical Research Council of Turkey (TÜBİTAK) research grant of ÇAYDAĞ-109Y044 and partly by the DEU-BAP Project: 2007.KB.FEN.039. We thank the guest editor (Dr. E. Bozkurt) and three anonymous reviewers for their constructive comments that greatly improved the manuscript.

References

Akartuna, M., 1962. İzmir-Torbalı-Seferihisar-Urla bölgesi jeolojisi hakkında (Geology of İzmir-Torbalı-Seferihisar-Urla region). Bulletin of the Mineral Research and Exploration of Turkey 59, 1–18.

Akay, E., Erdoğan, B., 2004. Evolution of Neogene calc-alkaline to alkaline volcanism in the Aliağa-Foça region (Western Anatolia, Turkey). Journal of Asian Earth Science 21, 367–387.

Akdeniz, N., Konak, N., Öztürk, Z., 1986. İzmir-Manisa dolaylarının jeolojisi [Geology of İzmir-Manisa surroundings]. Mineral Research and Exploration of Turkey, Report No: 7929.

Aksu, A.E., Piper, D.J.W., Konuk, T., 1987. Late quaternary tectonic and sedimentary history of outer İzmir and Çandarlı bays, western Turkey. Marine Geology 76, 89–104.

Aktuğ, B., Kılıçoğlu, A., 2006. Recent crustal deformation of İzmir, western Anatolia and surrounding regions as deduced from repeated GPS measurements and strain field. Journal of Geodynamics 41, 471–484.

Akyarlı, A., Arısoy, A., Er, T., 1988. Current and sea level measurements performed in the İzmir Bay. Proceedings of the Environmental Science and Technology Conference, İzmir, Turkey. Environment 1, 1–12.

Akyol, N., Zhu, L., Mitchel, B.J., Sözbilir, H., Kekovalı, K., 2006. Crustal structure and local seismicity in Western Anatolia. Geophysical Journal International 166 (3), 1259–1269, http://dx.doi.org/10.1111/j.1365-246X.2006.03053.x.

Alexandrowski, P., 1986. Graphical determination of principal directions for slickenside lineation populations: an attempt modify Arthaud's method. Journal of Structural Geology 7, 73–82.

Alpar, B., Burak, S., Gazioğlu, C., 1997. Effect of weather system on the regime of sea level variations in İzmir Bay. Turkish Journal of Marine Sciences 3, 83–92.

Anderson, E.M., 1951. The Dynamics of Faulting. Oliver & Boyd, Edinburgh, 206pp.

Angelier, J., 1979. Determination of the mean principal directions of stress for a given fault population. Tectonophysics 56, 17–26.

Angelier, J., 1984. Tectonic analysis of fault slip data sets. Journal of Geophysical Research 80, 5835–5848.

Angelier, J., 1990. Inversion of field data in fault tectonics to obtain the regional stress: III. A new rapid direct inversion method by analytical means. Geophysical Journal International 103, 363–376.

Angelier, J., 1994. Fault slip analysis and paleostress reconstruction. In: Hancock, P. (Ed.), Continental Deformation. Pergamon, Oxford, pp. 101–120.

Angelier, J., Dumont, J.F., Karamanderesi, İ.H., Poısson, A., Şimşek, Ş., Uysal, Ş., 1981. Analyses of fault mechanisms and expansion of southwestern Anatolia since the Late Miocene. Tectonophysics 79, 11–19.

Armijo, R., Carey, E., Cisternas, A., 1982. The inverse problem inmicrotectonics and the separation of tectonic phases. Tectonophysics 82, 145–169.

Armijo, R., Meyer, B., Hubert, A., Barka, A., 1999. Westwards propagation of the North Anatolian Fault into the Northern Aegean: Timing and kinematics. Geology 27, 267–270.

Arthaud, F., 1969. Méthode de determination graphique des directions de reccourcissement, d'allongement et intermédiaire d'une population de failles. Bulletin de la Societé Géologique de France 7, 729–737.

Benetatos, C., Kiratzi, A., Ganas, A., Ziazia, A., Plessa, A., Drakatos, G., 2006. Strike-slip motions in the Gulf of Sığacık (western Anatolia): properties of the 17 October 2005 earthquake seismic sequence. Tectonophysics 426, 263–279.

Bergerat, F., Angelier, J., Andreason, P., 2007. Evolution of paleostress fields and brittle deformation of the Tornquist Zone in Scania (Sweden) during Permo-Mesozoic and Cenozoic times. Tectonophysics 444, 93–110.

Borsi, S., Ferrara, G., Innocenti, F., Mazzuoli, R., 1972. Geochronology and petrology of recent volcanics in the eastern Aegean Sea (west Anatolia and Leovos Island). Bulletin of Volcanology 36, 473–496.

Bozkurt, E., 2001. Neotectonics of Turkey—a synthesis. Geodinamica Acta 14, 3–30.

Bozkurt, E., 2003. Origin of NE-trending basins in western Turkey. Geodinamica Acta 16, 61–81.

Bozkurt, E., Park, R.G., 1997. Microstructures of deformed grains in the augen gneisses of southern Menderes massif and their tectonic significance, western Turkey. Geologische Rundschau 86, 101–119.

Bozkurt, E., Satır, M., 2000. The southern Menderes Massif (western Turkey): Geochronology and exhumation history. Geological Journal 35, 285–296, doi:10.1002/gj.849.

Bozkurt, E., Sözbilir, H., 2004. Tectonic evolution of the Gediz Graben: field evidence for an episodic, two extension in western Turkey. Geological Magazine 141, 63–79.

Bozkurt, E., Sözbilir, H., 2006. Evolution of the large-scale active Manisa Fault, Southwest Turkey: implications on fault development and regional tectonics. Geodinamica Acta 19, 427–453.

Brahim, L.A., Chotin, P., Abdelouafi, A., El Adraoui, A., Nackha, C., Dhont, D., Charroud, M., Alaoui, F.S., Amrhar, M., Bouaza, A., Tabyaoui, H., Chaouni, A., 2002. Paleostress evolution in the Moroccan African margin from Triassic to Present. Tectonophysics 357, 187–205.

Candan, O., Dora, O.Ö., Oberhanslı, R., Çetinkaplan, M., Partzsch, J.H., Warkus, F.C., Dürr, S., 2001. Pan-African high-pressure metamorphism in the Precambrian basement of the Menderes Massif, Western Anatolia, Turkey. International Journal of Earth Science 89, 793–811.

Carey, E., Brunier, B., 1974. Analyse théorique et numérique d'une mode'le méchanique élémentaire appliqué a l'étude d'une population de failles. Comptes Rendus de l'Académie des Sciences Series D 279, 891–894.

Catlos, E.J., Baker, C., Sorensen, S.S., Çemen, İ., Hançer, M., 2010. Geochemistry, geochronology, and cathodoluminescence imagery of the Salihli and Turgutlu granites (central Menderes Massif, western Turkey): implications for Aegean tectonics. Tectonophysics 48, 110–130.

Çakmakoğlu, A., Bilgin, Z.R., 2006. Pre-Neogene stratigraphy of the Karaburun Peninsula (W of İzmir Turkey). Bulletin of the Mineral Research and Exploration of Turkey 132, 33–61.

Çiftçi, N.B., Bozkurt, E., 2008. Folding of the Gediz Graben fill, SW Turkey: extensional and/or contractional origin? Geodinamica Acta 21, 145–167.

Delvaux, D., Sperner, B., 2003. Stress tensor inversion from fault kinematic indicators and focal mechanism data: the TENSOR program. In: Nieuwland, D. (Ed.), New Insights into Structural Interpretation and Modelling, vol. 212. Geological Society, London, pp. 75–100 (Special Publications).

Doblas, M., 1998. Slickenside kinematic indicators. Tectonophysics 295, 187–197.

Emre, T., Sözbilir, H., 1997. Field evidence for metamorphic core complex, detachment faulting and accomodation faults in the Gediz and Büyük Menderes grabens (Western Turkey). International Earth Sciences Colloquium on the Aegean Region IESCA-95 I, 73–94.

Emre, T., Sözbilir, H., 2007. Tectonic evolution of the Kiraz Basin, Küçük Menderes Graben: evidence for compression/uplift-related basin formation overprinted by extensional tectonics in West Anatolia. Turkish Journal of Earth Science 16, 441–470.

Emre, Ö., Özalp, S., Doğan, A., Özaksoy, V., Yıldırım, C., Göktaş, F., 2005. İzmir Yakın Çevresinin Diri Fayları ve Deprem Potansiyelleri [The Active Faults of the İzmir Region and their Earthquake potentials]. Mineral Research and Exploration of Turkey, Report No: 10754.

Ercan, T., Satır, M., Kreuzer, H., Türkecan, A., Günay, E., Çevikbaş, A., Ateş, M., Can, B., 1985. Batı Anadolu Senozoyik volkanitlerine ait yeni kimyasal, izotopik ve radyometrik verilerin yorumu (Interpretation of the new geochemical, isotopic and radiometric age data from the western Anatolia Cenozoic volcanics). Bulletin of the Geological Society of Turkey 28, 121–136.

Ercan, E., Satır, M., Sevin, D., Türkecan, A., 1996. Batı Anadolu' daki Tersiyer ve Kuvaterner yaşlı volkanik kayaçlarda yeni yapılan radyometrik yaş ölçümlerinin yorumu (Some new radiometric ages from Tertiary and Quaternary volcanic rocks from West Anatolia). Bulletin of Mineral Research and Exploration Institute of Turkey 119, 103–112.

Erdoğan, B., 1990. Tectonic relations between İzmir–Ankara Zone and Karaburun Belt. Bulletin of Mineral Research and Exploration Institute of Turkey 110, 1–15.

Ersoy, E.Y., Helvacı, C., Sözbilir, H., 2010. Tectono-stratigraphic evolution of the NE–SW-trending superimposed Selendi basin: implications for late Cenozoic crustal extension in Western Anatolia, Turkey. Tectonophysics 488, 210–232.

Eşder, T., Şimsek, Ş., 1975. Geology of İzmir (Seferihisar) geothermal area western Anatolia of Turkey determination of reservoirs by means of gradient driling. In: Proceedings of 2nd UN, Symposium. San Francisco, pp. 349–361.

Etchecopar, A., Visseur, A., Daignieres, M., 1981. An inverse problem in microtectonics for the determination of stress tensors from fault striation analysis. Journal of Structural Geology 3, 51–65.
Fry, N., 1999. Striated faults: visual appreciation of their constraint on possible paleostress tensors. Journal of Structural Geology 21, 7–21.
Genç, S.C., Altunkaynak, Ş., Karacık, Z., Yılmaz, Y., 2001. The Çubukludağ Graben, Karaburun peninsula: it's tectonic significance in the Neogene geological evolution of the western Anatolia. Geodinamica Acta 14, 45–55.
Gephart, J.W., Forsyth, D.W., 1984. An improved method for determining the regional stress tensor using earthquake focal mechanism data. Journal of Geophysical Research B89, 9305–9320.
Gessner, K., Piazolo, S., Güngör, T., Ring, U., Kroner, A., Passchier, C.W., 2001. Tectonic significance of deformation patterns in granitoid rocks of the Menderes nappes, Anatolide belt, southwest Turkey. International Journal of Earth Sciences 89, 766–780.
Glodny, J., Hetzel, R., 2007. Precise U–Pb ages of syn-extensional Miocene intrusions in the central Menderes Massif, Western Turkey. Geological Magazine 144, 235–246.
Gürer, O., Sarica-Filoreau, N., Özburan, M., Sangu, E., Do!gan, B., 2009. Progressive development of the Büyük Menderes Graben based on new data, western Turkey. Geological Magazine 146, 652–673.
Hancock, P.L., Barka, A.A., 1987. Kinematic indicators on active normal faults in western Turkey. Journal of Structural Geology 9 (5/6), 573–584.
Hardcastle, K.C., Hills, L.S., 1991. BRUTE3 and SELECT: Quick Basic 4 programmes for determination of stress tensor configurations and separation of heterogeneous populations of fault slip data. Computer Geoscience 17, 23–43.
Heidbach, O., Tingay, M., Barth, A., Reinecker, J., Kurfess, D., Müller, B., 2010. Global crustal stress pattern based on the World Stress Map database release 2008. Tectonophysics 482, 3–15.
Helvacı, C., Ersoy, Y., Sözbilir, H., Erkül, F., Sümer, Ö., Uzel, B., 2009. Geochemistry and 40Ar/39Ar geochronology of Miocene volcanic rocks from the Karaburun Peninsula: implications for amphibole-bearing lithospheric mantle source, Western Anatolia. Journal of Volcanology and Geothermal Research 185, 181–202.
Hetzel, R., Ring, U., Akal, C., Troesch, M., 1995. Miocene NNE-directed extensional unroofing in the Menderes Massif, southwestern Turkey. Journal of the Geological Society of London 152, 639–654.
Hippolyte, J.-C., Mann, P., 2011. Neogene–Quaternary tectonic evolution of the Leeward Antilles islands (Aruba, Bonaire, Curaçao) from fault kinematic analysis. Marine and Petroleum Geology 28, 259–277.
Hippolyte, J.-C., Bergerat, F., Gordon, M.B., Bellier, O., Esput, N. Keys and pitfalls in mesoscale fault analysis and paleostress reconstructions, the use of Angelier's methods. Tectonophysics, in press.
Innocenti, F., Kolios, N., Manetti, P., Rita, F., Villari, L., 1982. Acid and basic late Neogene volcanism in central Aegean Sea: its nature and geotectonic significance. Bulletin of Volcanology 45, 87–97.
Işık, V., Seyitoğlu, G., Çemen, İ., 2003. Ductile–brittle transition along the Alaşehir detachment fault and its structural relationship with the Simav detachment fault, Menderes Massif, Western Turkey. Tectonophysics 374, 1–18.
Işık, V., Tekeli, O., Seyitoğlu, G., 2004. The Ar-40/Ar-39 age of extensional ductile deformation and granitoid intrusion in the northern Menderes core complex: implications for the initiation of extensional tectonics in Western Turkey. Journal of Asian Earth Sciences 23, 555–566.
Jolivet, L., Lecomte, E., Huet, B., Denèle, Y., Lacombe, O., Labrousse, L., Le Pourhiet, L., Mehl, C., 2010. The North Cycladic Detachment System. Earth and Planetary Science Letters 289, 87–104.
Kaya, O., 1979. Ortadoğu Ege çöküntüsünün (Neojen) stratigrafisi ve tektoniği (Neogene Stratigraphy and tectonics of the middle-east Aegean depression). Bulletin of the Geological Society of Turkey 22, 35–58.
Kaya, O., 1981. Miocene reference section for the coastal parts of West Anatolia. Newsletters on Stratigraphy 10, 164–191.
Kaymakçı, N., White, S.H., van Dijk, P.M., 2000. Paleostress inversion in a multiphase deformed area: kinematic and structural evolution of the Çankırı Basin (central Turkey), Part 1. In: Bozkurt, E., Winchester, J.A., Piper, J.A.D. (Eds.), Tectonics and Magmatism in Turkey and the Surrounding Area. Geological Society, London, pp. 445–473 (Special Publications 173).
Kaymakçı, N., White, S.H., van Dijk, P.M., 2003. Kinematic and structural development of the Çankırı Basin (Central Anatolia, Turkey): a palaeostress inversion study. Tectonophysics 364, 85–113.
Kaymakçı, N., İnceöz, M., Ertepınar, P., 2006. 3D-architecture and Neogene evolution of the Malatya Basin: inferences for the kinematics of the Malatya and Ovacık fault zones. Turkish Journal of Earth Sciences 15, 123–154.
Kaymakçı, N., Aldanmaz, E., Langereis, C., Spell, T.L., Gurer, O.F., Zanetti, K.A., 2007. Late Miocene transcurrent tectonics in NW Turkey: evidence from palaeomagnetism and $^{40}Ar-^{39}Ar$ dating of alkaline volcanic rocks. Geological Magazine 144 (2), 379–392.
Kiratzi, A., Louvari, E., 2003. Focal mechanisms of shallow earthquakes in the Aegean Sea and the surrounding lands determined by waveform modelling: a new database. Journal of Geodynamics 36, 251–274.
Koçyiğit, A., Özaçar, A.A., 2003. Extensional neotectonic regime through the NE edge of the Outer Isparta Angle, SW Turkey: New field and seismic data. Turkish Journal of Earth Sciences 12, 67–90.
Koçyiğit, A., Yusufoğlu, H., Bozkurt, E., 1999. Evidence from the Gediz Graben for episodic two-stage extension in western Turkey. Journal of the Geological Society London 156, 605–616.
Kozur, H., 1997. Pelagic Permian and Triassic of the western Tethys and its paleogeographic and stratigraphic significance. XLVIII. Bergund Hüttenmannisher Tag, Technische Universitat Bergakademie Freiberg, pp. 21–25 (Abstract book).
Krantz, R.W., 1988. Multiple fault sets and three-dimensional strain: theory and application. Journal of Structural Geology 10, 225–237.
Le Pichon, X., Chamot-Rooke, N., Lallemant, S., Noomen, R., Veis, G., 1995. Geodetic determination of the kinematics of central Greece with respect to Europe: Implications for Eastern Mediterranean Tectonics. Journal of Geophysical Research 100, 12675–12690.
Lips, A.L.W., Cassard, D., Sözbilir, H., Yılmaz, H., Wijbrans, J.R., 2001. Multistage exhumation of the Menderes Massif, western Anatolia (Turkey). International Journal of Earth Science 89, 781–792.
Lykousis, V., Anagnostou, C., Pavlakis, P., Rousakis, G., Alexandri, M., 1995. Quaternary sedimentary history and neotectonic evolution of the eastern part of Central Aegean Sea, Greece. Marine Geology 125, 59–71.
Maniatis, G., Hampel, A., 2008. Along-strike variations of the slip direction on normal faults: insights from three-dimensional finite-element models. Journal of Structural Geology 30, 21–28.
Marret, R., Allmendinger, R.W., 1990. Kinematic analysis of fault-slip data. Journal of Structural Geology 12, 973–986.
Marret, R., Peacock, D.C.P., 1999. Strain and stress. Journal of Structural Geology 21, 1057–1063.
Means, W.D., 1976. Stress and Strain. Springer-Verlag, New York.
Means, W.D., 1987. A newly recognized type of slickenside striation. Journal of Structural Geology 9, 585–590.
Michael, A.J., 1984. Determination of stress from slip data: faults and folds. Journal of Geophysical Research B89, 11517–11526.
Morris, A., Anderson, M., 1996. First paleomagnetic results from the Cycladic Massif, Greece, and their implications for Miocene extension directions and tectonic models in the Aegean. Earth and Planetary Science Letters 142, 397–408.
Ocakoğlu, N., Demirbağ, E., Kuşcu, İ., 2005. Neotectonic structures in İzmir Gulf and surrounding regions (western Turkey): evidences of strike-slip faulting with compression in the Aegean extensional regime. Marine Geology 219, 155–171.
Okay, A.İ., 2001. Stratigraphic and metamorphic inversions in the central Menderes Massif: a new structural model. International Journal of Earth Science 89, 709–727.
Okay, A.I., Altıner, D., 2007. A condensed Mesozoic section in the Bornova Flysch Zone: a fragment of the Anatolide-Tauride carbonate platform. Turkish Journal of Earth Sciences 16, 257–279.
Okay, A.İ., İşinteki İ., Altıner, D., Özkan-Altıner, S., Okay, N. An olistostrome-melange belt formed along a suture: Bornova Flysch zone, western Turkey, Tectonophysics, in press.
Okay, A.I., Satır, M., Maluski, H., Siyako, M., Monié, P., Metzger, R., Akyüz, S., 1996. In: Yin, A., Harrison, M. (Eds.), Paleo- and Neo-Tethyan events in northwest Turkey: geological and geochronological constraints. Tectonics of Asia, pp. 420–441.
Özer, S., Sözbilir, H., 2003. Presence and tectonic significance of Cretaceous rudist species in the so-called Permo-Carboniferous Göktepe formation, central Menderes Massif, western Turkey. International Journal of Earth Science 92, 397–404.
Özer, S., Sözbilir, H., Özkar, İ., Toker, V., Sarı, B., 2001. Stratigraphy of Upper Cretaceous-Paleocene sequences in the southern and eastern Menderes Massif. International Journal of Earth Science 89, 852–866.
Özgenç, İ., 1978. Cumaovası (İzmir) asitvolkanitlerde saptanan iki ekstrüzyon aşaması arasındaki göreceli yaş ilişkisi (Relative age relationships between two extrusion phases of Cumaovası acidic volcanics (İzmir)). Bulletin of the Geological Society of Turkey 21, 31–34.
Özkaymak, Ç., Sözbilir, H., 2008. Stratigraphic and structural evidence for fault reactivation: the active Manisa fault zone, western Anatolia. Turkish Journal of Earth Sciences 17/3, 615–635.
Özkaymak, Ç., Sözbilir, H., Uzel, B., 2011. Geological and palaeoseismological evidence for late Pleistocene-Holocene activity on the Manisa Fault Zone, western Anatolia. Turkish Journal of Earth Sciences 20, 1–26, doi:10.3906/yer-0906-18.
Özkaymak, Ç., Sözbilir, H., Uzel, B. Neogene-Quaternary Evolution of the Manisa Basin: Evidence for Variation in the Stress Pattern of the İzmir–Balıkesir Transfer Zone, Western Anatolia. Journal of Geodynamics, in press.
Pe-Piper, G., Piper, D.J.W., Kotopouli, C.N., Panagos, A.G., 1995. Neogene volcanoes of Chios, Greece. The relative importance of subduction and back-arc extension. Geological Society London 81, 213–232 (Special Publications).
Pe-Piper, G., Piper, D.J.W., Matarangas, D., 2002. Regional implications of geochemistry and style of emplacement of Miocene I-type diorite and granite, Delos, Cyclades, Greece. Lithos 60, 47–66.
Petit, J.P., 1987. Criteria for the sense of movement on fault surfaces in brittle rocks. Journal of Structural Geology 9, 597–608.
Petit, J.P., 1987. Determination of the tectonic stress tensor from slip along faults that obey the Coulomb yield criterion. Tectonics 6, 849–861.
Reilinger, R.E., Mcclusky, S.C., Vernant, P., Lawrence, S., Ergintav, S., Çakmak, R., Nadariya, M., Hahubia, G., Mahmoud, S., Sakr, K., Arrajehi, A., Paradissis, D., Al-Aydrus, A., Prilepin, M., Guseva, T., Evren, E., Dmitritsa, A., Filikov, S.V., Gomes, F., Al-Ghazzi, R., Karam, G., 2006. GPS constraints on continental deformation in the Africa-Arabia-Eurasia continental collision zone and implications for the dynamics of plate interactions. Journal of Geophysical Research 111, B05411, doi:10.1029/2005JB004051.

Ring, U., Susanne, L., Matthias, B., 1999. Structural analysis of a complex nappe sequence and late orogenic basins from the Aegean Island of Samos, Greece. Journal of Structural Geology 21, 1575–1601.
Ring, U., Johnson, C., Hetzel, R., Gessner, K., 2003. Tectonic denudation of a Late Cretaceous-Tertiary collisional belt: Regionally symmetric cooling patterns and their relation to extensional faults in the Anatolide belt of western Turkey. Geological Magazine 140 (4), 421–441, doi:10.1017/S0016756803007878.
Robertson, A.H.F., Pickett, E.A., 2000. Paleozoic–Early Tertiary Tethyan evolution of mélanges, rift and passive margin units in the Karaburun Peninsula (western Turkey) and Chios Island (Greece). In: Bozkurt, E., Winchester, J.A., Piper, J.D.A. (Eds.), Tectonics and Magmatism in Turkey and Surrounding Area. Geological Society, London, pp. 43–82 (Special Publications 173).
Saintot, A., Angelier, J., 2002. Tectonic paleostress fields and structural evolution of the NW-Caucasus fold-and-thrust belt from Late Cretaceous to Quaternary. Tectonophysics 357, 1–31.
Sarı, B. Late Maastrichtian–Late Palaeocene planktic foraminiferal biostratigraphy of the matrix of the Bornova Flysch Zone around Bornova. Turkish Journal of Earth Sciences, in press.
Sarıca, N., 2000. The Plio-Pleistocene age of Büyük Menderes and Gediz Grabens and their tectonic significance on N–S extensional tectonics in West Anatolia: mammalian evidence from the continental deposits. Geological Journal 35, 1–24.
Savaşçın, Y., 1978. Foça-Urla Neojen Volkanitlerinin Mineralojik ve Jeokimyasal İncelenmesi ve Kökensel Yorumu [Mineralogical and Geochemical Investigations and Source Interpretations of Foça-Urla Neogene Volcanites]. PhD Thesis, pp. 1–15.
Sayın, E., 2003. Physical features of the İzmir Bay. Continental Shelf Research 23, 957–970.
Sayın, E., Pazı, İ., Eronat, C., 2006. Investigation of water masses in İzmir Bay, western Turkey. Turkish Journal of Earth Sciences 15, 343–372.
Şengör, A.M.C., 1987. Cross-faults and differential stretching of hanging walls in regions of low-angle normal faulting: examples from Western Turkey. In: Coward, M.P., Dewey, J.F., Hancock, P. (Eds.), Continental Extensional Tectonics. Journal of the Geological Society, London, pp. 575–589 (Special Publications).
Şengör, A.M.C., Görür, N., Şaroğlu, F., 1985. Strike-slip faulting and related basin formation in zones of tectonic escape: Turkey as a case study. In: Biddle, K., Christie-Blick, N. (Eds.), Strike-Slip Deformation, Basin Formation and Sedimentation. Society of Economic Paleontologists and Mineralogists, pp. 227–264 (Special Publications 37).
Seyitoğlu, G., Çemen, İ., Tekeli, O., 2000. Extensional folding in the Alaşehir (Gediz) Graben, western Turkey. Journal of the Geological Society London 157, 1097–1100.
Seyitoğlu, G., Tekeli, O., Çemen, İ., Şen, Ş., Işık, V., 2002. The role of the flexural rotation/rolling hinge modeling the tectonic evolution of the Alaşehir graben, Western Turkey. Geological Magazine 139, 15–26.
Sözbilir, H., 2001. Extensional tectonics and the geometry of related macroscopic structures: field evidence from the Gediz detachment, western Turkey. Turkish Journal of Earth Sciences 10, 51–67.
Sözbilir, H., 2002. Geometry and origin of folding in the Neogene sediments of the Gediz Graben, Western Anatolia, Turkey. Geodinamica Acta 15, 277–288.
Sözbilir, H., Sarı, B., Akgün, F., Gökçen, N., Akkiraz, S., Sümer, Ö., Erkül, F., 2004. First example of a transtensional supradetachment basin in western Anatolia: The Kemalpaşa-Torbalı Basin, Turkey. In: Proceedings of the 32nd Internatinonal Geological Congress, Italy, p. 894 (Abstracts 2).
Sözbilir, H., Uzel, B., Sümer, Ö., İnci, U., Ersoy, Y.E., Koçer, T., Demirtaş, R., Özkaymak, Ç., 2008. Evidence for a kinematically linked E–W trending İzmir Fault and NE-trending Seferihisar Fault: Kinematic and paleoseismogical studies carried out on active faults forming the İzmir Bay, Western Anatolia (D-B uzanımlı İzmir Fayı ile KD-uzanımlı Seferihisar Fayı'nın birlikte çalıştığına dair veriler: İzmir Körfezi'ni oluşturan aktif faylarda kinematik ve paleosismolojik çalışmalar Batı Anadolu). Bulletin of the Geological Society of Turkey 51/2, 91–114.
Sözbilir, H., Kaymakçı, N., Langereis, C., Uzel, B., Özkaymak, Ç., Özkaptan, M., Gülyüz, M., 2009. Transfer zonlarının jeolojik evrimi ve bu zonların Batı Anadolu'daki K-G genişleme tektoniğine katkısı: İzmir–Balıkesir Transfer Zonu [Geological evolution of transfer zones and their contribution to N-S Extensional tectonics in western Anatolia: İzmir–Balıkesir Transfer Zone]. 13th Meeting of Active Tectonics Research Group, p. 51 (Abstracts).
Sözbilir, H., Sarı, B., Uzel, B., Sümer, Ö., Akkiraz, S., 2011. Tectonic implications of transtensional supradetachment basin development in an extension-parallel transfer zone: the Kocaçay Basin, western Anatolia, Turkey. Basin Research 23, 423–448, doi:10.1111/j. 1365-2117.2010.00496.x.
Sperner, B., Zweigel, P., 2010. A plea for more caution in fault–slip analysis. Tectonophysics 482, 29–41.
Sperner, B., Müller, B., Heidbach, O., Delvaux, D., Reinecker, J., Fuchs, K., 2003. Tectonic stress in the Earth's crust: advances in the World Stress Map project. Geological Society London 212, 101–116 (Special Publications).
Sümer, Ö., 2007. Güzelbahçe (İzmir) çevresinin alüvyonal sedimantolojisi ve aktif tektoniği [Alluvial sedimentology and active tectonics of Güzelbahçe (İzmir) surroundings]. M.Sc. Thesis, p. 114.
Tan, O. The dense micro-earthquake activity at the boundary between the Anatolian and South Aegean microplates. Journal of Geodynamics, in press.
Tan, O., Tapırdamaz, C., Yörük, A., 2008. The Earthquake catalogues for Turkey. Turkish Journal of Earth Sciences 17, 405–418.
Tatar-Ekrül, S., Sözbilir, H., Erkül, F., Helvacı, C., Ersoy, E.Y., Sümer, Ö., 2008. Geochemistry of I-type granitoids in the Karaburun Peninsula, West Turkey: evidence for Triassic continental arc magmatism following closure of the Palaeotethys. Island Arc 17, 394–418.
Taymaz, T., Yılmaz, Y., Dilek, Y., 2007. The geodynamics of the Aegean and Anatolia: introduction. In: Taymaz, T., Yılmaz, Y., Dilek, Y. (Eds.), The Geodynamics of the Aegean and Anatolia. Geological Society, London, pp. 1–16 (Special Publications 291).
Twiss, R.J., Moores, E.M., 1992. Structural Geology. W.H. Freeman, New York.
van Hinsbergen, D.J.J., 2010. A key extensional metamorphic core complex reviewed and restored: the Menderes Massif of western Turkey. Earth-Science Reviews 102, 60–76.
Walcott, C.R., White, S.H., 1998. Constraints on the kinematics of post-orogenic extension imposed by stretching lineations in the Aegean region. Tectonophysics 298, 155–175.
Uzel, B., Sözbilir, H., 2008. A first record of strike-slip basin in western Anatolia and its tectonic implication: the Cumaovası basin as an example. Turkish Journal of Earth Sciences 17, 559–591.
Uzel, B., Sözbilir, H., Özkaymak, Ç., 2012. Neotectonic evolution of an actively growing superimposed basin in western Anatolia: The inner bay of İzmir, Turkey. Turkish Journal of Earth Sciences 22 (4), 439–471, doi:10.3906/yer-0910-11.
Vandycke, S., Bergerat, F., 2001. Brittle tectonic structures and palaeostress analysis in the Isle of Wight, Wessex basin, southern UK. Journal of Structural Geology 23, 393–406.
Will, T.M., Powell, R., 1991. A robust approach to the calculation of paleostress fields from fault plane data. Journal of Structural Geology 13, 813–821.
Yamaji, A., 2000. The multiple inverse method: a new technique to separate stresses from heterogeneous fault-slip data. Journal of Structural Geology 22, 441–452.
Yin, Z.M., Ranalli, G., 1993. Determination of tectonic stress field from fault slip data, toward a probabilistic model. Journal of Geophysical Research 98, 12165–12176.
Zalohar, J., Vrabec, M., 2007. Paleostress analysis of heterogeneous fault-slip data: the Gauss method. Journal of Structural Geology 29, 1798–1810.
Zhu, L., Akyol, N., Mitchell, B.J., Sözbilir, H., 2006. Seismotectonics of western Turkey from high resolution earthquake relocations and moment tensor determinations. Geophysical Research Letters 33, L07316, doi:10.1029/2006GL025842.